

POLITECNICO DI MILANO

School of Industrial and Information Engineering

Master of Science in Biomedical Engineering



POLITECNICO
MILANO 1863

"Enhancing electrophysiological signal recording: innovations in optrode design and technology compared to standard measurement instrumentation"

Relatore: Carlo Ettore Fiorini

Relatori esterni: Amr Al Abed, Nigel Lovell

Monaco Ilaria 997111

Academic year 2022/2023

Acknowledgements

A special thanks to Dr. Amr, who promptly responded to my email seeking a multidisciplinary experience at UNSW. From our initial meeting at 6 a.m. (Italian time-zone), he has been constant in his support throughout this journey. I am deeply grateful for his patience, assistance, availability, and most importantly, his invaluable guidance, which have been fundamental to my progress. Furthermore, I express profound gratitude to Prof. Lovell for extending the opportunity to work at UNSW and for warmly welcoming me into his laboratory with great enthusiasm. I would also like to thank Prof. Fiorini, who without his approval this project could have been undertaken. Thanks for encouraging me to embark on this path, and even if from a distance, his presence was crucial for me.

Ringraziamenti

Un ringraziamento speciale a Dr. Amr, che ha risposto prontamente alla mia e-mail in cerca di un'esperienza di tesi all'estero presso UNSW. Dal nostro incontro iniziale alle 6 del mattino (ora italiana), è stato costante nel suo sostegno durante tutto il percorso. Gli sono profondamente grata per la sua pazienza, la sua assistenza, la sua disponibilità e, soprattutto, la sua preziosa guida, che sono state fondamentali per i miei progressi. Inoltre, esprimo profonda gratitudine al Prof. Lovell per avermi offerto l'opportunità di lavorare all'UNSW e per avermi accolto con grande entusiasmo nel suo laboratorio. Vorrei anche ringraziare il Prof. Fiorini, che senza la sua approvazione non avrei potuto impegnarmi in questo progetto. Lo ringrazio per avermi incoraggiato a intraprendere questo percorso e, anche se a distanza, la sua presenza è stata fondamentale per me.

Abstract

Advances in neurotechnology have led to the development of optical-electrode or optrode devices, promising tools for recording neural signals, thus overcoming certain constraints that traditional electrode suffers from, by converting signals from the electrical to the optical domain at the tissue interface. This project addresses critical challenges to minimise electrical stimulation artefacts during signal acquisition, optimise device packaging to mitigate stimulation artefacts and facilitate universal electrode compatibility. Experimental efforts focus on comprehensive electrical and optical characterisation of the sensor through benchtop evaluations and software refinement for precise measurements. In particular, the replication of several case studies from various neuroscience research projects was efficiently executed and meticulously analysed. Moreover, a new packaging of the optrode transducer has been realised, so called “OpBox,” whose term was coined from “optrode” and “box.” This was deemed necessary in order to reduce stimulation artefacts and to allow recording with different electrodes but with the use of a single optrode transducer as a universal 'headstage'. The absence of significant electrical ‘mains’ interference noise contamination in the OpBox recordings increases the reliability and robustness of the data for analysis. However, the design of the OpBox needs to be improved to ensure biocompatibility and flexibility, particularly for *in vivo* brain-machine interfaces. The resulting improvements and findings that I have achieved hold significant implications for future work and the fabrication of the next generation of optrode neurotechnology.

Sommario

I progressi della neurotecnologia hanno portato allo sviluppo di dispositivi opto-elettrodi o optrode, strumenti promettenti per la registrazione dei segnali neurali, superando così alcune limitazioni di cui soffre l'elettrodo tradizionale, convertendo i segnali dal dominio elettrico a quello ottico all'interfaccia del tessuto. Questo progetto affronta le sfide critiche per ridurre al minimo gli artefatti da stimolazione elettrica durante l'acquisizione del segnale, ottimizzare il confezionamento del sensore per attenuare gli artefatti da stimolazione e facilitare la compatibilità universale degli elettrodi. Gli sforzi sperimentali si concentrano sulla caratterizzazione elettrica e ottica completa del sensore e il perfezionamento del software per misure precise. In particolare, la replica di diversi casi di studio tratti da vari progetti di ricerca nel campo delle neuroscienze è stata analizzata meticolosamente ed eseguita in modo efficiente. Inoltre, è stato realizzato un nuovo packaging del trasduttore dell'optrode, cosiddetto "OpBox", il cui termine è stato coniato da "optrode" e "box", dove il transducer viene inserito. Ciò è stato ritenuto necessario per ridurre gli artefatti da stimolazione e consentire la registrazione con elettrodi diversi ma con l'uso di un trasduttore come 'headstage' universale. L'assenza di significative interferenze elettriche nelle registrazioni di OpBox aumenta l'affidabilità e la robustezza dell'analisi dei dati. Tuttavia, il design dell'OpBox deve essere migliorato per garantire biocompatibilità e flessibilità, in particolare per le interfacce cervello-macchina in vivo. I miglioramenti e i risultati ottenuti hanno implicazioni significative per il lavoro futuro e per la realizzazione della prossima generazione di neurotecnologie con optrodi.

Table of Contents

- List of Figures** 6
- List of Tables** 8
- Nomenclature** 9
- 1. Introduction** 10
- 2. State of the art** 12
 - 2.1 Single electrode..... 12
 - 2.2 Multi-electrode arrays 15
 - 2.3 Optical electrode..... 18
 - 2.3.1 Liquid-crystal operation principle and architecture 19
 - 2.4 Multi-optical arrays..... 24
 - 2.5 Design considerations..... 26
 - 2.5.1 Green electronics 28
 - 2.6 Artefacts considerations 29
- 3. Research objectives** 31
- 4. Materials and Method** 32
 - 4.1 Noise measurement..... 32
 - 4.2 New OpBox 34
 - 4.2.1 Design requirements..... 34
 - 4.2.2 First OpBox prototype..... 35
 - 4.2.3 Second OpBox prototype 38
 - 4.3 Case studies 39
 - 4.4 Experiments set up 41
 - 4.4.1 Nerve experiment 43

4.4.2 Cornea ring experiment	46
4.4.3 Artificial vision experiment	48
4.4.4 <i>Ex vivo</i> experiment	49
4.4.5 <i>In vivo</i> experiment	50
4.5 Software	52
5. Interpretation and Discussion of Results	54
5.1 Gain measurement	54
5.2 Case studies	58
5.2.1 Nerve experiment	58
5.2.2 Cornea ring experiment	61
5.2.3 Artificial vision experiment	64
5.3 <i>Ex vivo</i> Nerve experiment	65
5.4 <i>In vivo</i> Nerve experiment.....	67
6. Conclusions and future developments.....	74
Appendix A	77
Appendix B.....	78
References	79

List of Figures

Figure 1 Single electrode techniques.....	14
Figure 2 In vivo silicon-based 100 channel microelectrode array.....	16
Figure 3 Illustration of operating principle of electro-optical transducers utilising deformed helix ferro electric liquid crystals.....	21
Figure 4 Block diagram of the optrode recording system.....	23
Figure 5 Optrode array prototype.....	24
Figure 6 Process diagram for the fabrication of multi-optrode arrays.....	25
Figure 7 Single transducer cell.....	26
Figure 8 First OpBox prototype.....	35
Figure 9 Transducer set up within the first OpBox prototype.....	36
Figure 10 Second optrode packaging prototype.....	38
Figure 11 Optical connection and electrodes connection - universal plug for various electrode types.....	38
Figure 12 Block diagram gain measurement set up with unpackaged optrode and OpBox. .	42
Figure 13 Block diagram nerve experiment set up with standard measurement instrumentation.....	44
Figure 14 Block diagram experiment set up with optrode.....	45
Figure 15 Block diagram of the cornea ring experiment setup with standard measurement instrumentation.....	47
Figure 16 Block diagram of the artificial vision experiment setup with standard measurement instrumentation.....	49
Figure 17 PSD of unpackaged optrode and OpBox.....	57
Figure 18 Nerve benchtop experiment.....	59
Figure 19 Benchtop experiment using the Nerve case. Control measurements.....	60
Figure 20 Cornea benchtop experiment.....	61
Figure 21 Zoomed- in view cornea benchtop experiment.....	62
Figure 22 Benchtop experiment using the cornea ring case. Control measurements.....	63
Figure 23 Ex vivo nerve benchtop experiment.....	65

Figure 24 Zoomed- in view ex vivo nerve benchtop experiment.. 66

Figure 25 In vivo sciatic nerve experiment. Measured responses to a 1 mA, 1ms biphasic stimulus in a rat..... 68

Figure 26 In vivo sciatic nerve experiment. Measured responses to a 0.5 mA, 1ms biphasic in a rat. 69

Figure 27 In vivo sciatic nerve experiment. Measured responses to a 1.5 mA, 200 μ s biphasic stimulus pulse in a rat. 71

Figure 28 In vivo sciatic nerve experiment. Measured responses to a 0.5 mA, 200 μ s biphasic stimulus pulses in a rat.. 72

Figure 29 Artificial vision benchtop. Standard measurement instrumentation..... 78

List of Tables

Table 1 Recording and Stimulating electrodes for multiple user cases.....	40
Table 2 Unpackaged optrode and OpBox baseline noise standard deviation.....	56
Table 3 Unpackaged optrode and OpBox SNR.....	56
Table 4 Baseline analysis nerve experiment.	60
Table 5 Baseline analysis cornea ring experiment.....	63
Table 6 Artefact analysis for the 1 mA, 1ms biphasic pulse stimulus case.	69
Table 7 Artefact analysis for the 0.5 mA, 1ms biphasic stimulus case.	70
Table 8 Artefact analysis for the 1.5 mA, 200 μ s biphasic stimulus case.	71
Table 9 Artefact analysis for the 0.5 mA, 200 μ s biphasic stimulus case.	72
Table 10 LCs characteristics	77

Nomenclature

ADC	Analog-to-digital converter
BCI	Brain computer interface
BMI	Brain machine interface
CMOS	Complementary metal-oxide-semiconductor
CTE	Coefficient of thermal expansion
DAQ	Data acquisition hardware device
DBS	Deep-brain stimulation
DHF-LC	Helix ferroelectric liquid crystal
EMI	Electromagnetic interference
EP	Electrophysiology
FC	Fibre optic
GRIN	Gradient index optics
GSBME	Graduate School of Biomedical Engineering
HFS	High frequency stimulus
ITO	Indium tin oxide
LC	Liquid crystal
MEA	Multi-electrode array
MOA	Multi-optrode array
PD	Photodetector
PDMS	Polydimethylsiloxane
PDS	Power spectrum density
PM	Polarisation-maintaining
RGC	Retinal ganglion cell
SLD	Super-luminescence diode
SM	Single mode
SNR	Signal to noise ratio
UNSW	University of New South Wales

1. Introduction

Electrophysiological (EP) studies permit the measurement of ionic currents across the cell membrane, from single cells, or tissues. This group of techniques helps to understand the physiological and pathophysiological functions of excitable cells and tissue [1]. Measuring EP signals has a prominent role in monitoring patients' health. Techniques such as electrocardiology make extensive use of electrodes to measure the heart's electrical activity, allowing clinicians to detect abnormalities in cardiac health. Neurophysiology is another example of clinical electrophysiology: measurement of electrical properties of the brain, spinal cord, and nerves allow the diagnosis and monitoring of neurological diseases.

EP is often used in Brain Machine Interfaces (BMIs) techniques to record neural activity from the brain, which may provide fundamental assistive tools for people who suffer from motor and/or sensory deficits. Recently, this expectation has been upgraded to reflect the possibility that BMIs may also become a new neurorehabilitation therapy that takes advantage of the phenomenon of brain plasticity to induce partial neurological recovery in severely disabled patients [2].

With the growing influence of technology within the biomedical space, the need for more powerful and accurate techniques of recording EP signals is an ever-growing focus. Over the last century, the field of electrophysiology has primarily relied on arrays of metal electrodes—a wires-based technology. Multi-electrode arrays (MEAs) are the current state of the art electrophysiology technique for brain computer interface (BCI) or brain machine interface (BMI) applications. The history of BMIs is intimately related to the effort of developing new electrophysiological methods to record the extracellular electrical activity of large neuronal populations using multi-electrode configurations [2]. The data collected by BMIs at its most rudimentary form is an extracellular potential [3], generated by the electrochemical processes that occur in neurons or cardiac or muscle cells upon depolarisation and repolarisation of the cell during an action potential. Recent progress includes advances in

complementary metal-oxide-semiconductor (CMOS) design and microfabrication, which has enabled MEAs with high channel count and a high channel packing density [4] as well as the development of materials for improved tissue-device interfaces [5]. However, as these devices are wire-based they all suffer from the same limitations which will be briefly discussed in later sections. For these reasons, our main goal is to develop fundamentally new tools and technologies to better acquire and analyse EP signals. The introduction of optical-based technologies is a new frontier in electrophysiology, since they are considered as an alternative approach using light to sense and transmit the EP signals. Optical electrodes (optrodes) have overcome certain constraints that traditional electrode suffers from, by converting signals from the electrical to the optical domain at the tissue interface. Even so, there is much more development and testing required to match current conventional electrode systems. The objective of this thesis is to try to characterise and reduce the artefacts signals that are still affecting the EP signals recorded using optrodes, that may stem from, but are not limited to light sources, monitoring equipment issues and/or utility frequency (50 Hz and 60 Hz), but particularly stimulation artefacts when stimulating and recording from tissues or cells at the same time. Furthermore, a better design of the optrode sensor may improve the previous issue, in particular this thesis will focus on the redesign of the sensor packaging to enable connection to a wide variety of EP electrodes. The future possibility of having an implantable optrode sensor built with biocompatible materials and no-wires solutions could be understudy, but this would be out of the scopes of this thesis.

In the next sections, an introduction of the necessary background knowledge will be done, discussion of the state-of-the-art technological development, the methods used to achieve research objectives will be shown and explanation of the motivation behind the work done will be given. Then results will be presented and, a few considerations about results and further development of the device will be discussed.

2. State of the art

2.1 Single electrode

One of the first methods used in neuroscience to measure EP signals is based on single-electrodes.

Single electrode techniques are used to record the electrical activity of a single cell. The most common single electrode technique is intracellular recording, which involves inserting a microelectrode into the cell to measure the voltage across the cell membrane. Intracellular recording involves measuring voltage and/or current across the membrane of a cell. To make an intracellular recording, the tip of a fine (sharp) microelectrode must be inserted inside the cell, so that the membrane potential can be measured. Intracellular recording techniques have further subtypes, such as:

- Intracellular sharp/blind technique: This technique involves injecting a current into an excitable cell and measuring the resulting voltage change across the membrane. It is used to study how cells respond to different stimuli.
- Patch clamp: This technique is used to study individual ion channels in neurons. It involves attaching a glass micropipette to a neuron's membrane and applying suction to create a tight seal between the pipette and membrane. This allows researchers to record the electrical activity of individual ion channels.
- Voltage clamp (sub-type of patch clamp technique): it is used to study how ion channels in neurons work. It involves clamping the voltage across a neuron's membrane at a specific level and measuring the resulting current flow.
- Current clamp (sub-type of patch clamp technique): In current-clamp mode, the user injects a known current amplitude to the inside of the cell through their setup and observes the change in cellular excitability in response to these current injections.

Instead, extracellular recording techniques are a type of electrophysiological technique that record the electrical activity of excitable cells outside the cell membrane [6]. These techniques can be classified into three categories: field potential recordings, and single-unit recordings.

- Field potential recordings are extracellular recordings that measure the electrical activity of a group of cells in a volume of tissue.
- Single-unit recordings are extracellular recordings that measure the electrical activity of a single cell. [7]

The equipment required for performing these experiments varies depending on whether they are performed *in vivo*, *ex vivo*, or *in vitro*. The basic requirements for an extracellular recording setup include different types of electrodes, apparatus for controlling electrode position and placement, recording equipment, signal output, data analysis, and histological confirmation of recording sites usually required for *in vivo* recordings [6], [7]. This requirement is a limitation in EP, since a different amplifier or headstage (devices that are used to amplify and filter signals, which contains an amplifier chip, support components, and a connector to mate with a recording electrode) for each type of electrode are required, therefore another issue refers to the compensation for difference in electrode impedance.

In *Figure 1* a representation of the different types of single electrode techniques and their subtypes, which could help the reader to better visualise them.

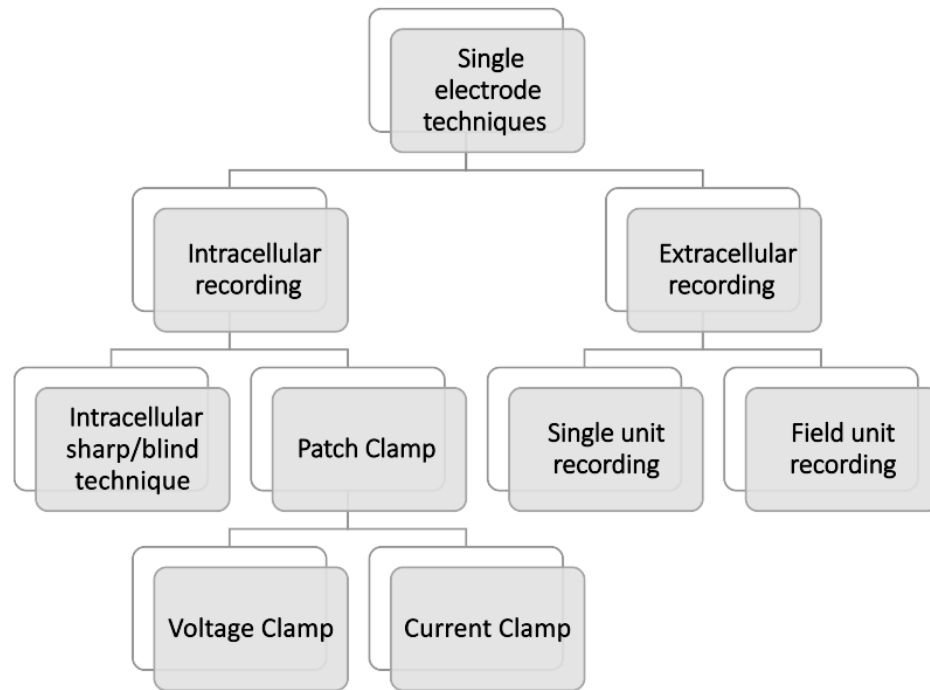


Figure 1 Single electrode techniques.

Single electrode techniques, both intracellular and extracellular have allowed researchers to discover the role of different parts of the brain in function and behaviour, therefore it permits the analysis of human cognition and cortical mapping. This information can then be applied to BMI technologies for brain control of external devices [8]. The workflow consists in inserting the microelectrode into the brain, where it can record the change in voltage with respect to time. Each technique has its own advantages and disadvantages, and the choice of technique depends on the experimental requirements.

For instance, In the sharp technique, which uses intracellular microelectrodes, you proceed slowly with the electrode, monitoring the potential until you insert the electrode into the cell. This contrasts with the patch-clamp technique, which uses glass microelectrodes, where you need a microscope to view a cell and the way you approach it is different and a seal needs to be made at the cell membrane before breaking it to enter. Here the disadvantage is the invasiveness of the technique because the cell membrane could be damaged but at the same time allow a high spatial resolution and a high signal-to-noise ratio (SNR), because electrode

noise is positively related to electrode impedance, and lower electrode impedance usually relies on a lower SNR. There is always a trade-off between the size of the electrode and the noise: lower noise is typically produced by increasing the effective size of the active tip [9].

Instead, in case of single unit recording techniques (extracellular recording) a major limitation can be the recording setup or rig and the electrical equipment used for measurement of channel activity. If the recording rig is not adequately isolated from vibrational or electrical noise, one runs the risk of not being able to observe single-channel events. The integrity of cell membrane or artificial bilayer can severely impact observations as well, as can the presence of contaminating chemicals and compounds. For these reasons and more, single-channel recording must be performed in a tightly controlled environment free from the multitude of factors that can make analysis difficult. However, single-channel recording permits high-resolution measurement of unique channel events. One can see discrete jumps in conductance as the channel opens and a return to the former conductance when the channel closes. One can also see both the duration of channel opening and closing as well as the frequency of channel gating. Channel blockage due to exogenous compounds as well as potential de-activation due to channel over stimulation (a behaviour of certain voltage-gated channels) can be observed [10].

2.2 Multi-electrode arrays

Historically, application of single-electrode extracellular recordings has been proven successful in experimentally measuring variance across a subject's electrical brain activity [11]. The issue with this method, however, lies in the limited range of cells that can be analysed during any single recording session and thus data compilation can take a long time. This led to the rise and development of MEAs as a measurement technique for both *in vitro* and *in vivo* experiments.

In vitro MEA technology has evolved into a widely used and effective methodology to study cultured neural networks. For this project *in vivo* MEA knowledge base will be more relevant, since in the case of *in vivo* experiments, MEAs are implantable and are currently the industry standard for multichannel neural and cardiac recording, with their development in the 1950's contributing to a surge in motivation for exploring neural recording and the application of such signals. Implantable neural MEAs (depicted in *Figure 2*) consist of an array of micro electrodes that contain a high number of channels (hundreds to thousands as of recent) that can be implanted on the cortex. This provides a high spatial resolution due to the electrode size and allows for recording local field potentials. MEAs are a powerful tool for recording biopotentials from excitable cells and tissue. They have been applied in electrophysiology research to map the sequential electric activation of cardiac tissue as well as neural cells and networks, to study the spatio-temporal evolution of synaptic connections, and in pharmacological and toxicological studies to assess the effect of chemicals on impulse excitation and propagation [12]. Smaller electrode areas allow higher density and channel count thereby enabling addressing of a larger number of cells [13]. The growing need for high spatial resolution in mapping excitation of neuronal and cardiac signals has seen the characteristics of MEA's improve drastically over the past 30 years, with factors such as electrode density, channels, speed, and SNR being the main targets for improvement.

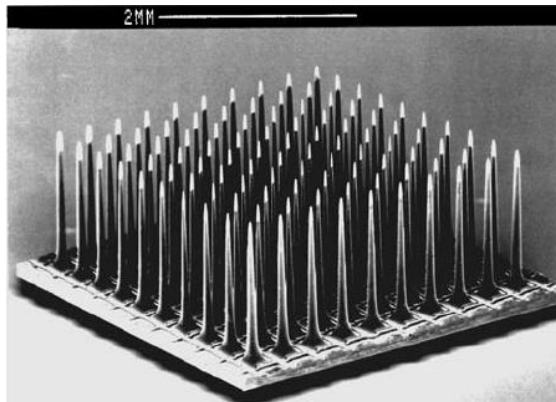


Figure 2 In vivo silicon-based 100 channel microelectrode array.

MEAs contain multiple (tens to thousands) microelectrodes of variable sizes, depending on several factors: the nature of the medium in which the cell or cells are located (e.g. the medium's electrical conductivity, capacitance, and homogeneity); the nature of contact between the cells and the MEA electrode (e.g. area of contact and tightness); the nature of the MEA electrode itself (e.g. its geometry, impedance, and noise); the analog signal processing (e.g. the system's gain, bandwidth, and behaviour outside of cutoff frequencies); and the data sampling properties (e.g. sampling rate and digital signal processing) [14]. However, when electrode size decreases and electrode-electrolyte bilayer impedance increases, the ratio of the input impedance to the total system impedance will decrease significantly, since lower is the electrode impedance higher is the SNR. To address some of these issues, Complementary Metal Oxide Semiconductor (CMOS) technology has been employed in MEA fabrication [15]. CMOS technology is a method to fabricate small custom integrated circuits and electronic chips. By integrating circuitry on the same substrate as the recording electrodes, CMOS MEAs can overcome some of the inherent limitations of passive MEAs. Most importantly, CMOS MEAs allow for overcoming the connectivity problem so that thousands of microelectrodes can be arranged at high spatial resolution through using multiplexing techniques, whereby electronic switches are employed to access shared signal wires. This approach drastically reduces the number of required interconnections between electrodes and amplifiers, thus allowing for a more effective use of available routing area. By integrating the amplifiers and analog-to-digital converters (ADCs) on the same substrate as the electrodes, the number of off-chip connections can also be reduced, since the digitised signals can be sent off-chip sequentially through only a small number of connections. Moreover, since the signals are amplified and filtered close to the signal source, the influence of noise picked up during signal transmission is minimised. However, CMOS MEAs developed so far are limited either in noise performance, since it might get an increase of noise because of all the electronics on the substrate, spatial resolution, or suffer from a comparably low readout channel count.

Modern MEAs still have drawbacks that limit their functionality and force them to rely on extraneous circuitry and recording apparatus, in order to successfully acquire a clean signal. At present different headstages or different amplifiers are required for each type of electrode, leading to cumbersome measuring set up. Furthermore, in addition to the impedance

mismatch problem, MEAs technology share one recording and signal transfer technique: electrical recording with conductive wiring could be a problem, in terms of space. In healthcare, challenges of hermetic encapsulation, and packaging and managing the multitude of leads required to transfer signals from the biological interface to data processing systems [16] are still present. Therefore, separating the geometric size of the electrode from the system circuitry hardware remains an unsolved problem.

2.3 Optical electrode

Recently, an alternative approach using light to sense and transmit the EP signals was developed by the research team of Graduate School of Biomedical Engineering (GSBME), UNSW, Sydney, NSW, Australia cooperating with the School of Electrical Engineering and Telecommunications, UNSW, Sydney, NSW, Australia. Liquid crystal (LC)-based optical electrodes for use as biopotential transducers are a unique proposal in replacement of current conventional single electrode arrays and MEAs. Optical-electrode (optrode) arrays use light to modulate excitable biological tissues and/or transduce bioelectrical signals into the optical domain. Light offers several advantages over electrical wiring, including the ability to encode multiple data channels within a single beam. This approach is at the forefront of innovation aimed at increasing spatial resolution and channel count in multichannel electrophysiology systems [17] Advantages include trackless design, immunity to impedance mismatching and electromagnetic interference, as well as label-free detection [12], [18]. Another main advantage is the use of optical fibres to carry the information, as the transfer of data through fibre optics is faster than through electrical wires, with lower loss and less electromagnetic interference [19]. Hence in general, reducing electrical connection will reduce noise and the acquisition system can even be much further away from the tissue [12], in contrast to the use of MEAs, where acquisition instrumentation needs to be as close as possible to reduce electrical wire length and possibility of power line interference. Regarding high density, signal multiplexing could easily be achieved by using different light wavelengths

for different channels, and carrying this information in a single optical fibre, thus reducing the electrical wiring issue of traditional MEAs [12].

2.3.1 Liquid-crystal operation principle and architecture

The optrode sensing mechanism is based on the conversion of extracellular biopotentials as generated by nerve, cardiac or muscle impulses into optical signals, utilising the anisotropic properties of LCs.

The basic transduction principle takes advantage of deformed helix ferroelectric (DHL) LCs which, under the presence of an external potential, realign, changing their light transmission properties. As such, when polarised light is shone through an LC layer, the amount of polarised transmitted light is proportional to the potential present.

Recent research on liquid crystals has demonstrated their remarkable responsiveness to electrical signals, with response times ranging from milliseconds to microseconds [20]. This rapid response is crucial for optrode devices, where quick modulation of optical properties is necessary. In many applications, especially in neuroscience and biomedical research, real-time monitoring of neural activity is essential to capture dynamic changes in brain or tissue function, especially given the millisecond nature of neuronal response. Fast response times enable optrode devices to quickly detect and transmit neural signals, allowing researchers to observe and analyse neural activity in real-time. Rapid modulation of optical properties ensures that the optrode device accurately represents the neural signals it detects. A slow response time could lead to delays or distortions in signal transmission, potentially compromising the fidelity of the recorded data.

The response time of LCs in transducers can depend on the specific type of LCs used. Different LC materials exhibit varying response times due to their molecular structure and properties. For instance, some factors that can influence the response time of LCs in transducers are:

- Type of liquid crystal: different types of LCs, such as nematic, smectic, and cholesteric LCs, have distinct response characteristics. For example, nematic LCs typically have faster response times compared to other types.
- Molecular alignment: the alignment of LC molecules within the transducer cell plays a crucial role in determining response time. The method used to align LC molecules, such as rubbing, photoalignment, or alignment layers, can impact how quickly the LCs respond to changes in voltage or external stimuli.
- Viscosity: the viscosity of the LC material affects its ability to reorient in response to an applied electric field. Lower viscosity LCs generally exhibit faster response times compared to higher viscosity ones.
- Temperature: LC response time is often temperature dependent. Changes in temperature can influence the viscosity and molecular mobility of the LC material, affecting its response dynamics.
- Presence of additives: The inclusion of additives or dopants in the LC material can modify its response characteristics. For example, certain additives may enhance or hinder the response time depending on their chemical properties.
- Cell design: the design of the LC transducer cell, including factors such as cell gap, electrode configuration, and alignment layers, can impact the response time by affecting the applied electric field and LC reorientation dynamics.[16]

More deeply in *Figure 3A* and in *Figure 3B* it is shown the sensing optrodes' principle of operation. When no electric field is applied, the average orientation of the deformed helix ferroelectric liquid crystal (DHF-LC) molecules sandwiched between two conductive substrates exhibits a helical structure whose axis lies in the cell's plane and whose orientation in that plane is dictated by alignment layers deposited on the inner surfaces of the substrates. If an electric field is built up between the surfaces, the molecular dipole moments will tend to align with it, thus deforming the helical structure. At the macroscopic level (*Figure 3C*), this deformation produces a rotation of the optical axes by an angle which, for small fields, is proportional to the strength of the applied electric field. A polarised light enters the LC layer, the amount of polarised light transmitted through is proportional to this rotation of the optical axes.

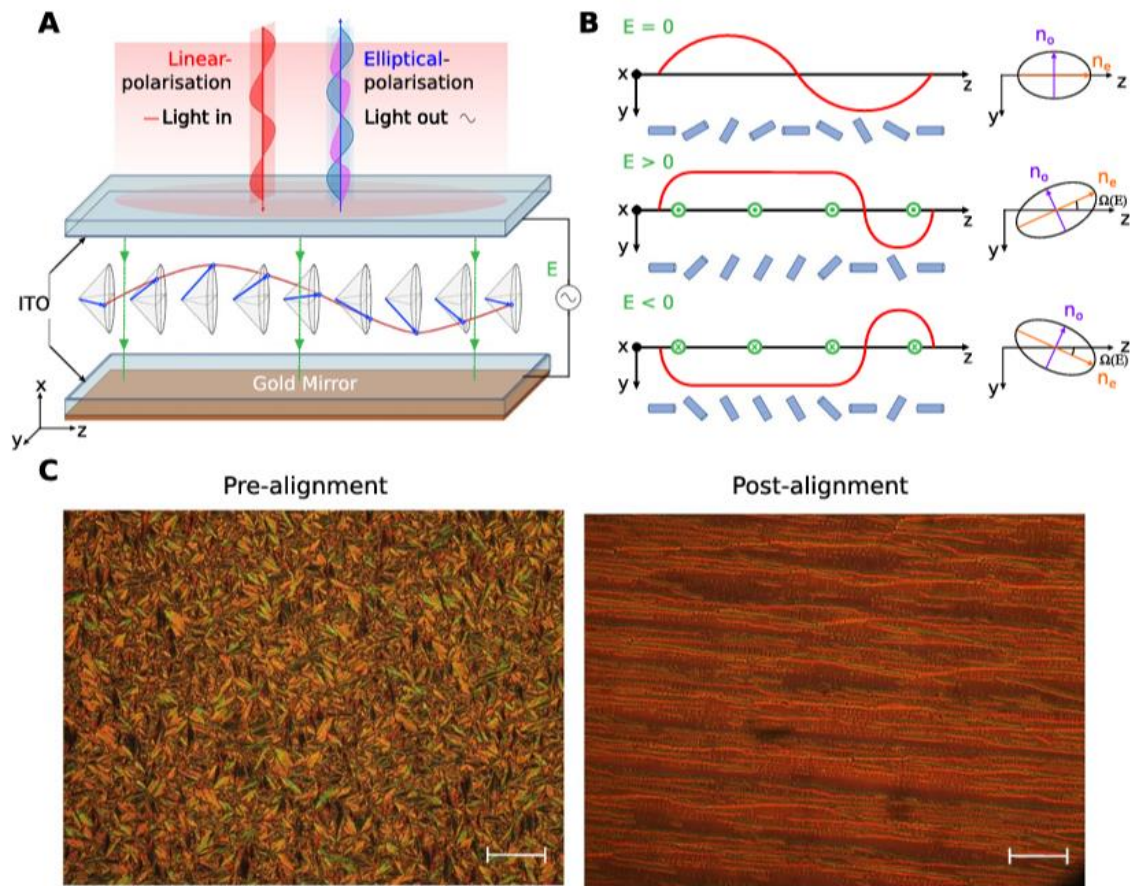


Figure 3 from [19] Optrode transducers. (A), (B) Illustration of operating principle of electro-optical transducers utilising deformed helix ferro electric liquid crystals. (A) Microscopic view of liquid crystal arrangement in a helix structure and the light polarisation state changing with the applied electric field, E . (B) Schematic of deformed helix structure of liquid crystals, represented by cylinders, in the presence of electric fields. (C) Representative microscopy images showing an example of unaligned and aligned liquid crystal domains.

Figure 4B explains in a more schematic way how light enters the optrode. It is from a mathematical modelling paper [12], before any experimental measurements were done. Said so, thanks to further development the basic set up still the same, the only difference is that, nowadays instead of a single mode (SM) light beam and a polariser, needed for the light polarisation, polarisation-maintaining (PM) fibres are used, without the linear polariser, because they provide greater stability to the entire system. The schematic cross-section of

the single channel optrode device used in the second possible configuration with PM fibres is illustrated in *Figure 4C*. This setup is less sensitive to fibre bending and to vibrations in general, which can increase the signal to noise ratio (SNR) in practical circumstances. However, considering a microscope setup (i.e., no optical fibre but using a light beam), then a linear polariser would be required to polarise the light beam originating from the microscope 's light source and align the resulting polarised light beam at the optimal angle relative to the LC optical axis. For this project, the transducer utilised is PM fibre coupled. Consequently, the following configuration will be considered. Electro-optical transducers were fabricated by sandwiching a 5 μm thick layer of DHF-LC between two ≈ 0.7 mm thick indium tin oxide (ITO)-coated glass substrates of empty LC cells. A gold mirror was attached to the exterior face of one ITO-glass substrate (*Figure 5*). Gold was chosen as a reflective layer due to its excellent reflectance ($\approx 98\%$) at 1550 nm. The ITO and gold layer were connected to metal pins for the application of electric potentials. ITO is an optoelectronic material that is applied widely in both research and industry. It has the distinguishing feature of being highly transparent and electrically conductive, therefore it serves as the connective layer to create the voltage difference across the LC layer. It is important to consider that the ITO and the physiological solution are connected via one of the metal pins and a reference ground electrode.

Proceeding with the optrode operating principle, which can be better visualised in *Figure 4A*, polarised light is delivered to the optrode devices, via PM fibres, from a super-luminescence diode (SLD). PM fibres assure the polarisation of the light; therefore, polarised light (1550 nm) is delivered using a polarisation maintaining (PM) fibre with a 10.5 μm diameter core, via a gradient-index lens and quarter-wave plate, which converts the linear polarisation into elliptical or circular polarisation before passing through the DHF-LC transducer. Specialised DHF-LCs can smoothly, continuously, and passively transduce electrical signals into the optical domain [16]. Gradient index lenses (GRINs) are built into the optrode architecture as a collimator function, which narrows the light beam leaving the PM fibre toward the gold channel, where the light must enter. When the light is reflected through the DHF-LC layer by the transducer's rear-mounted mirror and coupled back into the same PM fibre, the DC-

coupled photodetector firstly records the signal when the transducer is connected to a signal generator or excitable biological tissue, for conversion into an electrical signal and acquisition.

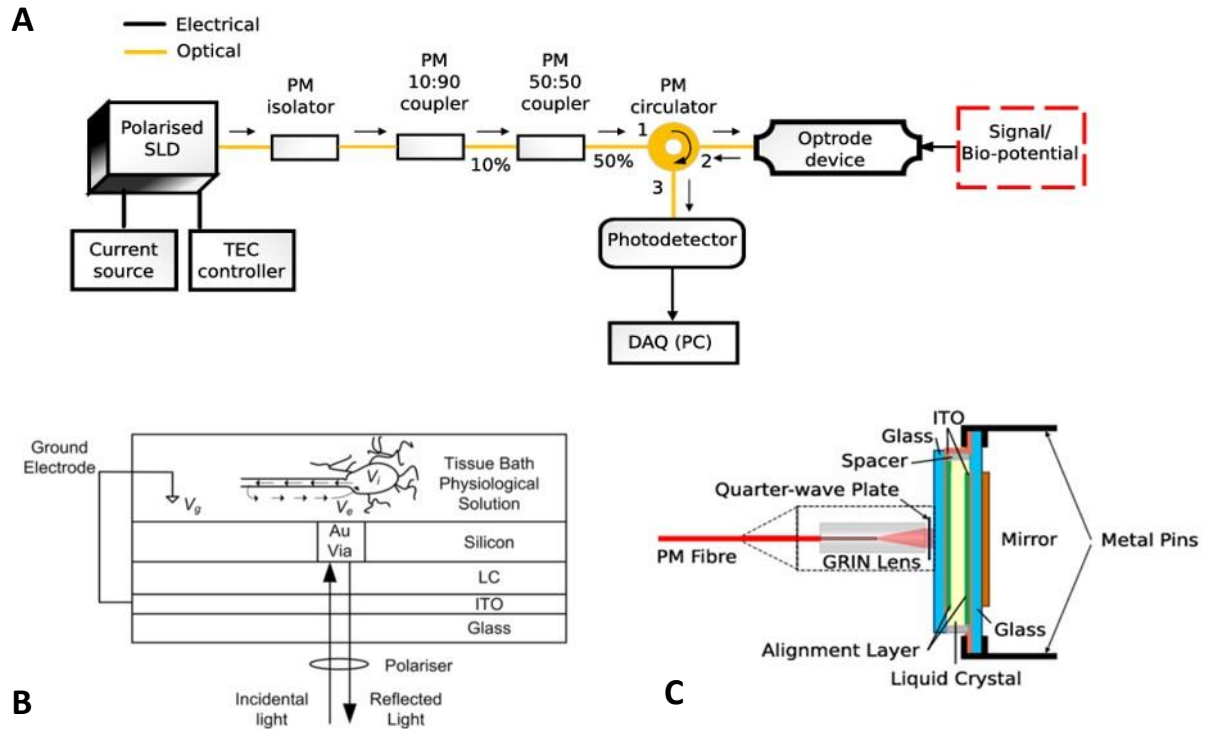


Figure 4 (A) taken from [16] Block diagram of the optrode recording system. A fibre-based optical setup is used to deliver light to the optrode device. The optrode transduces biopotentials into a light signal, which is then routed to a photodetector for conversion into an electrical signal and acquisition. (B) taken from [12]. Schematic of an optical transducer composition. (C) taken from [16] cross-section and photo of a single channel optrode device. Schematic dimensions are not scaled.

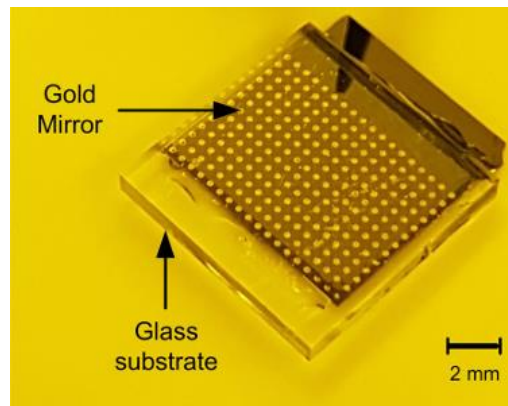


Figure 5 taken from [11]. Optrode array prototype. 300 gold mirrors for 300 distinct sensing sites.

2.4 Multi-optical arrays

Thanks to the collaboration between the GSBME and the School of Electrical Engineering and Telecommunications of the UNSW, Multi-optical arrays (MOAs) were fabricated using a similar architecture to the single channel optrode device described above, but the back substrate with the mirror was replaced with a more complex structure. This process is illustrated in *Figure 6*.

MOAs overcome the limitation of current recording systems by using light to carry bioelectric signals and overcome the single-optrode limitation regarding the acquisition of signals from unique cells.

The development of MOAs is proposed to lead to the next generation of BCI. It enables high-density, high channel count recording from neural and cardiac tissue.

Successful applications have to be demonstrated and have been tested by the multi-disciplinary team composed by GSBME and the School of Electrical Engineering and Telecommunication members of the UNSW, such as: demonstrate ability to map electrical activation in hearts in animal models and demonstrate ability to record peripheral nerve responses in animal models.

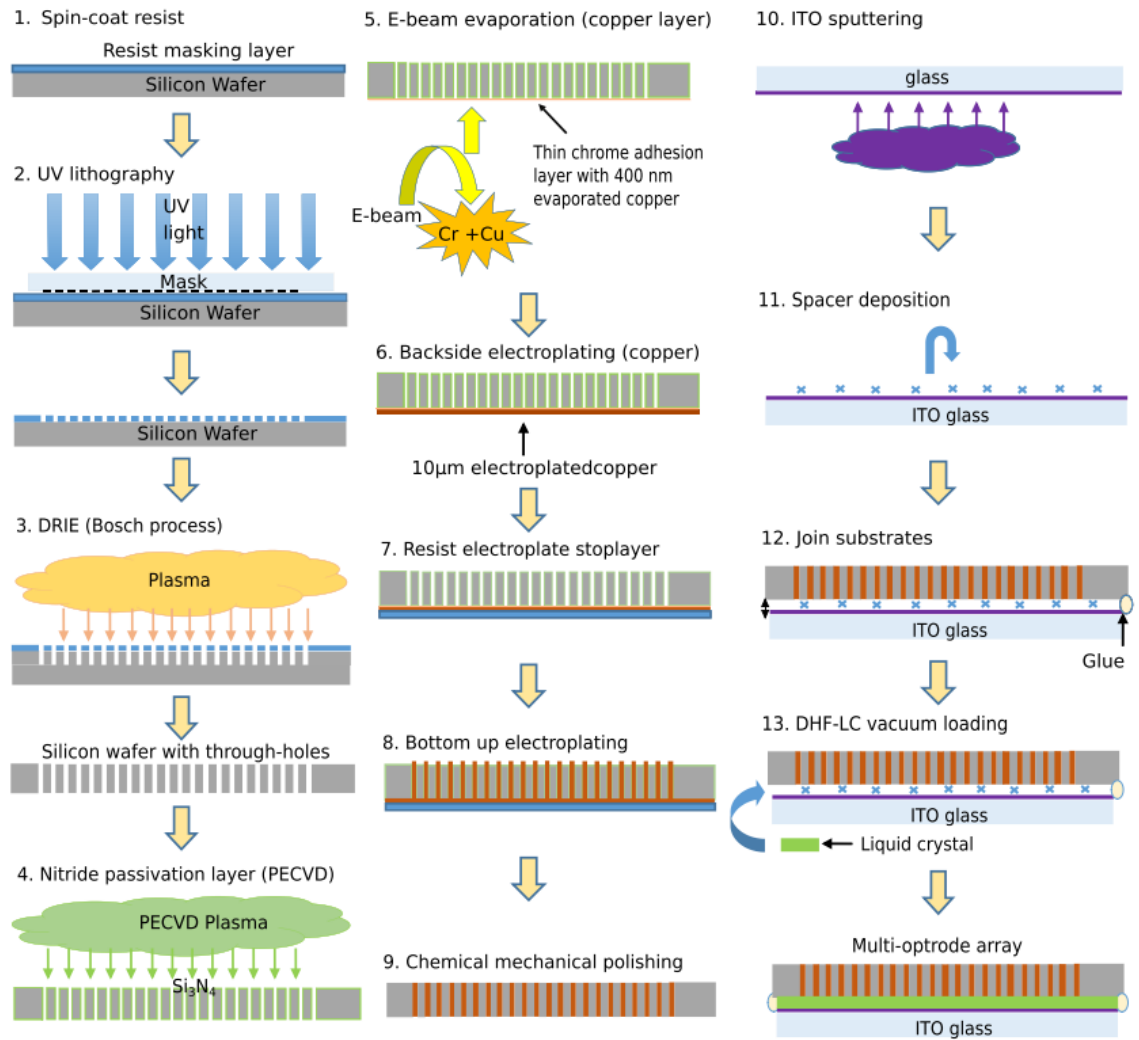


Figure 6 taken from [16] Process diagram for the fabrication of multi-optrode arrays. UV, ultra-violet; DRIE, deep reactive-ion etching; PECVD, plasma-enhanced chemical vapour deposition; ITO, indium tin oxide; DHF-LC, deformed helix ferroelectric liquid crystals.

2.5 Design considerations

In *Figure 7* it is presented how the optrode cell with all components is packaged within a metallic protective cap.



Figure 7 Single transducer cell. Voltage can be applied at the differential leads (pins). Size of the sensing area = 0.3 cm^2 .

The optrode device is only applicable for industrial purposes. To make it also applicable in the biomedical field, biocompatible materials must be considered. Currently, the material used for the optrode transducer cap is Kovar 4J29, a nickel-iron-cobalt alloy known for its low coefficient of thermal expansion (CTE). It is commonly used in applications where a tight seal is required between different materials over a wide temperature range, especially in electronic and electrical components. However, Kovar is not a biocompatible material, which means that if the optrode is to be implanted in the future, the material of the transducer cap must be modified, or new solutions must be found. Flexibility is another material characteristic that has been investigated, which could lead to better performance during EP signals acquisition. To advance the biomedical field, there is a need to develop flexible and soft variants of traditionally rigid photonic circuits for passive optical multiplexing. An evaluation of fabrication techniques against these requirements has been carried out in [17].

Other studies, to better design a conformal optrode, took inspiration from current applications of liquid-crystal displays (LCDs): the recent advancements in LC technology have seen substrates commonly being replaced with bendable, plastic substrates in order to promote flexibility. A study completed by Chen et al. [21] evaluated the efficacy of aligning LCs onto a flexible polydimethylsiloxane (PDMS) substrate using the replica moulding method. The method involved utilises a three-step process of dropping, curing, and peeling of the PDMS substrate and was chosen for its minimal fabrication cost and capability for mould re-use. Most importantly however, the replica moulding method allowed for duplication of the flexible constituent materials that current MEA production methods such as electron beam lithography fail to possess. Further testing completed within the study highlighted the feasibility of the substrate material in terms of transmission performance. It was seen that the transmittance of the LC cell, under conventional LCD voltages, are similar but not identical in rigid and flexed states. Chen et al. attributed this slight change due to the occurrence of cell gaps during bending and as the conductive layer was not changed, more flexible alternatives should be tested in future studies [21]. Although the LCD configuration featured in the work by Kim et al. displayed evidence of superior mechanical properties to current flexible LCDs, it was found that connection between the substrate and alignment layer was relatively weak [22]. These studies highlight the heavy variance in manufacturing methods used in creating more optimal flexible LCDs. However, the studies shown above focus primarily on the use of a PDMS substrate and thus it is unaware if other, more effective flexible materials currently exist as further research is to be completed. Studies have also been completed in attempting to develop potential replacements for currently used ITO films within electronics. A study completed by Yu et al. [23] investigated the use of ultrathin, flexible graphene films for use in supercapacitor applications by examining transmittance and absorbance rates of the device. Similar work has been completed by Yin et al. [24] that aimed to assess the potential use of reduced graphene-oxide (RGO) films on a PET substrate as replacement transparent electrodes. Although these studies show the vast opportunities of developing a flexible device for use in neural recordings, it is unclear if certain key parameters, such as impedance and transmittance, will be affected by the replacement of conventional electrodes with a multi-layered structure involving LCs. The above-mentioned articles provide a plethora of potential methods and materials that can be utilized in the optical electrode,

however limitations in the electro-optical and specifically mechanical characteristics of these techniques restrict immediate implementation.

Ultimately, another design considerations regards the sensing area of the optrode. At present, the only sensing area is the surface of the two rigid pins, which is a somewhat restrictive considering the variety of connection points where the device can be used. One solution to this limitation could be to have a universal plug that allows electrodes of different characteristics to be used according to application needs. Improving the quality of the device design could improve the quality of the recorded EP signals, which are nevertheless affected by unwanted artefacts. Artefact considerations will be discussed in another section.

2.5.1 Green electronics

“Green” electronics represents not only a novel scientific term but also an emerging area of research aimed at identifying compounds of natural origin and establishing economically efficient routes to produce synthetic materials that have applicability in environmentally safe (biodegradable) and/or biocompatible devices [25]. A key prerequisite for achieving sustainability in the electronics industry is the usage of materials and technologies that have low embodied energy, that is, products that consume a small amount of energy to be manufactured. Therefore, it uses less energy during its life cycle, resulting in fewer resources consumed to extract the raw material, produce specific parts, and transport the product.

Research in the emerging class of “green” electronics can help realise the original promise of organic electronics that are composed of energy-efficient materials and devices. Looking at biocompatible and biodegradable materials for the optrode device would be a revolutionary solution to its packaging design. In [25] biocompatible and biodegradable low-cost natural substrates have been investigated, such as shellac and hard gelatine. Shellac by itself is not inherently conductive but becomes so when combined with other materials in the ink formulation. In contrast, gelatine-based systems have been studied for their conductivity in

various applications. The conductivity of gelatine depends on the specific ingredients and preparation methods. However, it is important to note that hard gelatine capsules are mainly used to encapsulate drugs and supplements, rather than for their conductive properties. Combinations of these materials could be used for the future development of optrode sensor packaging. However, at the moment one of the goals of the project is to have a better design to reduce signal artefacts that are still present during EP signal acquisition, so experimenting with these different types of 'green' materials is outside the scope of this thesis.

2.6 Artefacts considerations

EP artefacts are undesired signals that can introduce changes in the measurements and affect the signal of interest. They can be broken down into three different categories: electrical, physiological, and environmental. Electrical artefacts are what will be covered, since they consist in measured cardiac potentials that are not related to electrical activity of the heart or in the case of neural stimulation, is any voltage difference signals that do not arise from neurons. Electrical devices used in the clinical setting can induce artefacts by various mechanisms. In [26] it is explained how electrode artefacts are an intrinsic property of the conductive electrodes of a lead. An electrode-intrinsic mechanism meaning a phenomenon that is an inescapable physical consequence of the electrode design, inherent to the geometry and materials of the electrode, and independent of electrical action, connection or loading of associated electronics [26]. Electrical efforts to minimise artefact tails in neuromodulation systems are important and ongoing [27]. Artefacts are a big issue in the neuroscience research and close-loop bionics, as the large stimulus artefact often overlaps and hides part of the biological response. Nowadays, removal techniques for the stimulation artefacts have been investigated: in [28] a proposed method provides an approach for real-time removal in closed-loop deep-brain stimulation (DBS) applications, where the artefact peaks were detected by applying a threshold to the raw recordings, and the samples within the contaminated period of the stimulation pulses were excluded and replaced with the

interpolation of the samples prior to and after the stimulation artefact duration. This method was evaluated with both simulation signals and *in vivo* closed-loop DBS applications in Parkinsonian animal models [28]. In [29], a hybrid methodology was presented as the combination of the two main methodological approaches for rejecting ocular artefacts from electroencephalographic (EEG) and magnetoencephalographic (MEG) signals: regression- and Blind Source Separation (BSS)-based techniques, both having merits, as well as some serious limitations. The BSS method includes a variety of unsupervised learning algorithms without prior information and extra reference channels. The main advantages of these two methods were combined, and it was assumed that the artefactual independent components (IC) extracted by the BSS method included more ocular activity and less brain activity than the contaminated EEG signals. Another method known as Independent Component Analysis (ICA), assuming that signal sources are instantaneously linear mixtures of cerebral and artefactual sources, can decompose observed signal into independent components (ICs). Once ICs are extracted from original signals, the clean signal is reconstructed by discarding ICs containing artefacts [30]. A similar technique is the use of blanking amplifiers. The working principle is based on the hypothesis that the stimulus artefact will saturate the amplifier. Hence the amplifier is controlled to be turned off (or blanked) during the delivery of the stimulus pulse so it does not get saturated. Even so, if the blanking technique is employed, the signals during the “blinking” period cannot be recorded and thus some important neural information may be missed [31]

However, the main goal in neuroscience is to avoid these artefacts from both the stimulation and recording site, without the necessity of any removal techniques. Demonstrating that the optrode device can reduce them it will be of huge benefit.

3. Research objectives

The optrode device showed similar recording capabilities compared to conventional bio-amplifiers. Improvements in the signal-to-noise ratio, sensing bandwidth, minimising artefacts, and relative responsivity to enable the detection of small variations in the nerve response are required. However, current iterations of this device prove to be insufficient for implantation within biological substances due to their rigid structure. Assessment of suitable replacement materials is minimal and thus further research is required.

The specific objectives of this projects regard:

- Minimising the optrode signals artefacts that still present during EP signal acquisition.
- Design: Improving the packaging of the sensor to reduce stimulation artefacts and to allow recording with different electrodes but with the use of the one optrode transducer as a universal 'headstage.'
- Experimental: Benchtop electrical and optical characterisation of sensor, including development of measurement instrumentation and software.
- Analytical: signal and image processing and statistical analysis of measured signals.

4. Materials and Method

4.1 Noise measurement

Preceding the development of a new packaging design, it is necessary to carry out a measurement with the optrode transducer itself in order to understand how much additional noise is caused by the transducer itself independent of the light source. In this way, it would be possible to visualise the margin of improvement that could be achieved.

To do so, a high-performance data acquisition hardware (DAQ) PowerLab (ADInstruments, ANZ) was used, and two different measurements were carried out:

1. Control measurement: alligator clips connected to the PowerLab DAQ and shortened.
2. Alligator clips connected to the two pins of the transducer.

In this first scenario the ideal case (low resistance scenario with shortened clips) is compared to that with the transducer. Ideally, the noises that are picked up from the optrode transducer should be lowered down to the levels obtained in the control measurement.

For both measurements, an analysis of the signal was conducted using MATLAB software (Mathworks, USA) and standard metrics to analyse the signals were used, such as average voltage, standard deviation, and power spectrum density (PSD).

The PSD provides valuable information about a signal's frequency content and how the signal's power is distributed across different frequency components. Analysing the PSD of a signal can reveal several insights:

- Frequency components: The PSD shows the different frequency components present in the signal. Peaks in the PSD indicate dominant frequencies in the signal. In this way, it is possible to identify the fundamental frequency and harmonics if they exist.
- Power distribution: The PSD tells you how the power is distributed across the frequency spectrum. It indicates which frequencies carry more or less power. This is essential for understanding the relative importance of different frequency components in the signal.
- Noise and interference: The PSD can help you identify noise and interference in the signal. These typically appear as random, broadband components in the PSD.
- Filter design: In case of the necessity to filter or process the signal, understanding the PSD can help to design appropriate filters, targeting specific frequency bands for enhancement or attenuation.
- System characterisation: In signal processing and communication systems, the PSD is used to characterise the behaviour of systems in the frequency domain. It is a critical tool in understanding how a system responds to different frequencies.
- Signal quality: The shape and characteristics of the PSD can provide insights into the quality of a signal.

4.2 New OpBox design

In the following sections, when discussing the updated optrode packaging the designation OpBox will be used. The term is coined from the term “optrode” and “box” (where the transducer is housed) in order to assign a more commercially oriented name.

4.2.1 Design requirements

One of the main objectives of this project is to improve the packaging of the optrode transducer to reduce stimulation artefacts and to allow recording with different electrodes but with the use of one optrode transducer as a universal ‘headstage.’ To this end, investigations were made into how conventional headstages are constructed, with the aim of trying to reproduce something similar with optrode transducers.

Another aspect that was deemed essential to address is the implementation of a multi-registration set-up package, to better eliminate artefacts. One optrode transducer will be connected to the recording electrode and its return electrode positioned at the point of interest for recording the signal, the other transducer will be connected to the same type of electrodes, but these will still be positioned away from the recording point of interest. In this way, through signal processing techniques such as subtraction, the artefact can be removed from the signal of interest.

4.2.2 First OpBox prototype

Figure 8 shows the first packaging design for the optrode transducers. An electromagnetic shielding box (EMI) made of aluminium is used as the main container. EMI has been proven to be an effective way to reduce the presence of electromagnetic interferences from the surrounding environment, and aluminium is light and has good conductivity. The optical connection is made on the left side of the box, which is then directly connected to the photodetector via an optical circulator, while the electrical connection is on the right side of the box, providing accessibility for plugging in various electrodes.

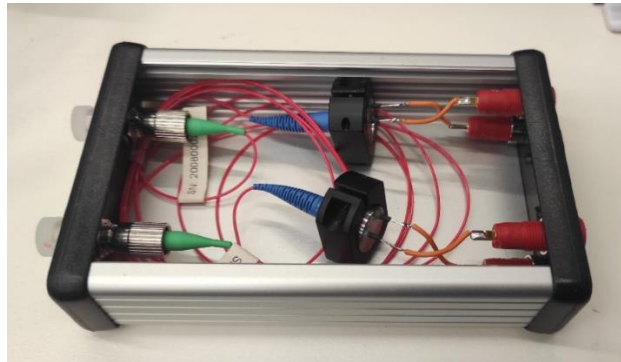


Figure 8 First OpBox prototype.

As for the optical part, two holes were drilled to insert the optical connector. The optical connector used is a single-mode fibre-optic (FC) adapter (see Appendix A for further technical details) and allows light to enter the optical fibres, connected to the transducer. It can be seen from *Figure 9* how the optrode transducer was fixed to the box in order to minimise any possible movement of the components during signal acquisition. Any movement or vibration of components can introduce noise and instability into the acquired signal. For this purpose, ring mount components were used (Appendix A) and each transducer was manually inserted and clamped inside a mounting ring.

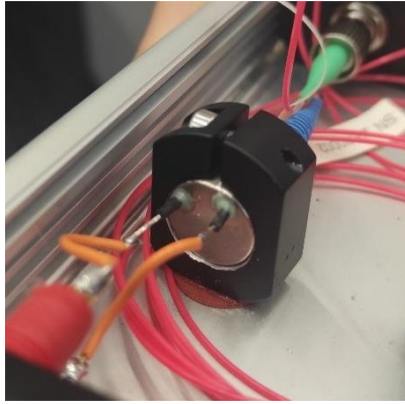


Figure 9 Transducer set up within the first OpBox prototype.

As far as the electrical connection is concerned, four holes were created to four gold-plated female banana sockets (Appendix A). The socket functions as an interface between the optrode transducer and all the different types of electrodes that each experiment may require. In this way, a universal socket is created. Gold plating was preferred because of its high electrical conductivity. It allows efficient and low-resistance transfer of electrical signals. The high conductivity of gold helps maintain a reliable and stable electrical connection. In addition, gold is highly resistant to corrosion.

In addition, the two pins of the transducer were soldered with a conductive wire to the gold plating of the pins to allow the electrical signal to be conducted. Finally, four male banana plugs, with gold plating (Appendix A) will be inserted in the four female socket to facilitate the insertion of each electrode.

After the first prototype a few observations were made, and these were fundamental for the development of a better prototype. To enable the box to be closed and keep the components inside it isolated from the external environment, sufficient clearance between the transducer mounting ring and the top surface of the box must be considered. For this reason, a box with a greater height is used for the second prototype. However, the box maintains the same characteristics as the first prototype box due to the properties explained above.

Considerations were made regarding the optical fibres. Optical fibres are typically designed to be quite fragile, and excessive bending can compromise their physical integrity. Furthermore, closing or bending optical fibres beyond a certain limit can lead to several

issues, and it is generally advisable to avoid excessive bending. This could cause signal attenuation, which means a loss of signal strength. The light signals transmitted through the fibre can scatter and leak out when the fibre is bent too tightly. This can result in a decrease in the quality and strength of the optical signal. To avoid these issues, it is important to respect the specified minimum bending radius. The minimum bending radius is the tightest curve that the fibre can safely tolerate without significant signal degradation or risk of damage. To prevent optical fibres from breaking, it is important to position them below the optical and electrical connections, so that they remain at the bottom of the box, without interacting with the top cover.

Finally, it is important to highlight that each transducer has different characteristic, the one that will be used for the following experiments is the TPM-I311-20080005. A characterisation was conducted previously by the research group in UNSW [16]. Its bandwidth is 10520 Hz, meaning that the device can accurately respond to signals with frequencies ranging from 0 Hz up to 10520 Hz, appropriate to record neural signals. See Appendix A for full characterisation report table.

4.2.3 Second OpBox prototype

For the second optrode packaging, as mentioned before, a bigger box (13 x 8 x 4 cm) is used in order to have higher clearance and enough room for the optical fibres, avoiding excessive bending, and consequently signal distortion.



Figure 10 Second optrode packaging prototype.

As it is visible in *Figure 10* the box could be completely isolated and this will help in avoiding electromagnetic interference from the environment.

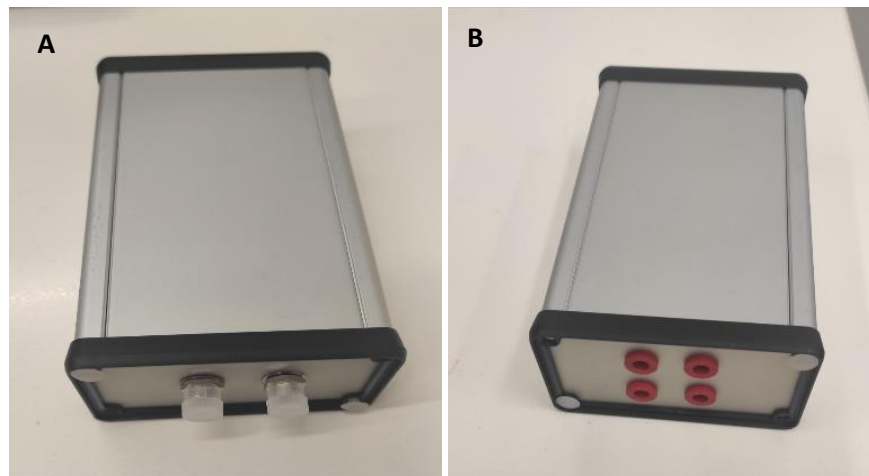


Figure 11 (A) Optical connection. (B) Electrodes connection - universal plug for various electrode types.

4.3 Case studies

To come up with a better design and better understand the problems most neuroscience researchers face during their experiments, several end-users were interviewed, in order to understand the various application scenarios.

The following three different studies recruited are running at UNSW in the School of Medical Sciences, Faculty of Medicine and in the School of Biomedical Engineering and are explained below in order to better understand their research areas.

1. Electrical stimulation in the nerve: the aim of this study is to characterise and model the neural effects of invasive and non-invasive nerve stimulation in human and rat peripheral nerve, considering the hypothesis that electrical stimulation will impede action potential generation at lower stimulation frequencies compared to mechanical stimulation. Using a novel delivery system developed by A/Prof Richard Vickey , deliver ultra-low frequency direct current (DC) stimulation in rat (invasive) and human (non-invasive) to increase the dynamic range of neural responses, could lead to create a significant improvement in the development and understanding of electrical stimulation approaches to restore touch sensations and treat chronic pain (unpublished manuscript [32])
2. Measuring brain activity following hybrid electrical/optical stimulation of the eyes: clinical trials of retinal optogenetic transfection have shown some success in achieving artificial vision, but exposing the retina to high intensity light long-term may be of concern. The aim of this study is to assess simultaneous electrical and optical (hybrid) stimulation as a method to reduce energy requirements, and its potential as an artificial vision treatment [33].
3. Electrical stimulation for artificial vision: this study focuses on characterising the response of four major functionally different retinal ganglion cells (RGCs) to a high frequency stimulus (HFS) paradigm [34]. *In vitro* patch clamp experiments have been done to assess the viability of evoking a differential response between different RGC types under a wide range of HFS and stimulation amplitude combinations because

different electrical stimulation waveforms have differing modes of activation based on intrinsic properties of the neurons. Patch clamping is used as it provides an irrefutable means of observing single-unit activity with relatively high recording quality, even in the presence of stimulation artefacts.

In the following paragraphs, the above three studies will be referred as: “Nerve experiment,” “Cornea ring experiment,” “Artificial vision experiment” respectively, for simplicity and compactness.

For all the studies a focus on the different type of recording and stimulating electrodes that have been used is done, reported, and visually represented in the following *Table1*.



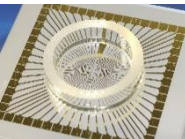
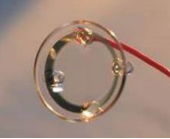
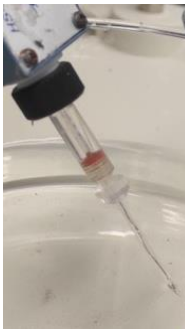

Studies	Recording electrode	Stimulating electrode
Nerve experiment	Monopolar hook electrode 	Surface electrodes 
Cornea ring experiment	Multi-channel electrode array 	Cornea ring electrode 
Artificial vision experiment	Monopolar patch pipette 	Single platinum electrode 

Table 1 Recording and Stimulating electrodes for multiple user cases.

4.4 Experiments set up

All the case studies were replicated first using the unpackaged optrode transducer and then using the new OpBox. This will not affect the measurement system circuit, as the OpBox contains the optrode transducer within it and plays the same role in detecting the stimulus signal.

In addition, a gain and baseline noise analysis were performed using the unpackaged optrode and OpBox to ensure that the new design would not affect signal acquisition. For this purpose, a sinusoidal function (2 V amplitude, 25 Hz frequency) was supplied from the DAQ (40 kHz sampling rate), as a stimulus signal directly to the unpacked optrode transducer pins, through alligator clips, and then, to test the OpBox, the same sinusoidal signal was supplied via the two plugs on the box, which are internally connected to the optrode pins. Following the optical path, highlighted in red in *Figure 12*, light from the light source (Thorlabs controller CLD1015, 1550 nm SLD) is transmitted to the optrode transducer via the circulator. The applied electrical signal causes a change in the polarisation of the light inside the optrode. The modulated light signal is then transmitted back to the circulator, and then into the PD (Thorlabs PDA10CS2). Thus, once the optical signal is converted into an electrical signal, amplification has been done (PD Gain: 30) to make the signal more detectable. Then, the electrical signal generated by the photodetector goes to a DAQ, for digitalisation and further software analysis.

Here the light source and PD settings that have been used in all the analysed case studies:

- Light controller current: 300 mA
- Light controller temperature: 20 °C
- PD Gain: 30

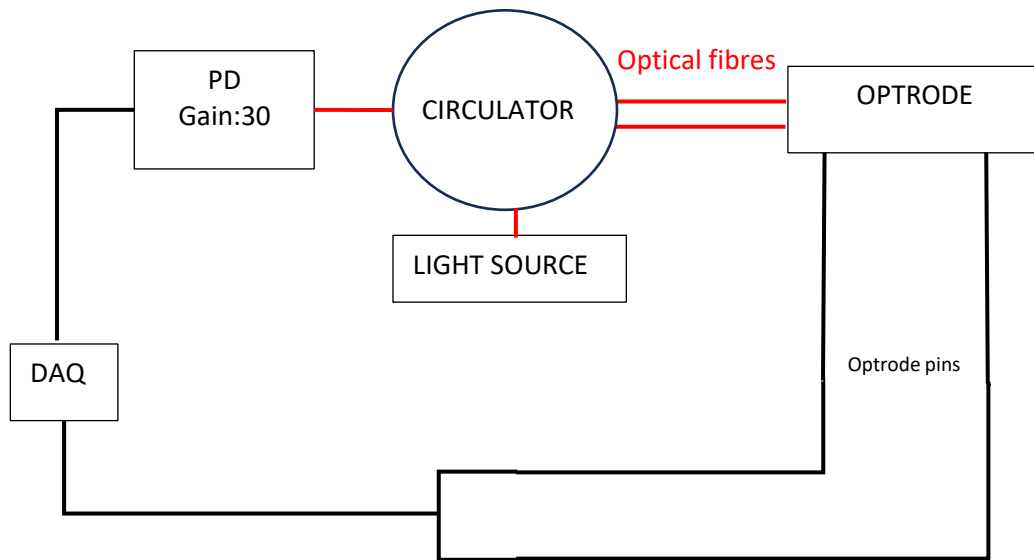


Figure 12 Block diagram gain measurement set up with unpackaged optrode and OpBox.

In the upcoming sections, a series of experiments will be conducted to assess the performance of the OpBox in comparison to traditional measurement instrumentation. These experiments will involve replicating the three user scenarios discussed above. Each of them will be replicated in a saline environment. In addition, the nerve experiment, will be followed by assessments using nerve tissue post-mortem. Within each scenario, comparisons will be drawn between unpackaged transducers and the OpBox configuration. Through these comparisons, valuable insights into the OpBox's effectiveness in minimising artefacts and improving signal fidelity across diverse experimental conditions will be gained.

It is important to emphasise that the positions of the electrodes remain constant throughout the experiments, with minimal deviation, particularly in the artificial vision case where they are nearly fixed. This consistency ensures that any disparities observed are solely attributable to differences between the recording systems rather than variations in the relative positions of the recording and stimulating electrodes. This clarification underscores the reliability of the comparisons made between the different recording configurations and their respective performances.

4.4.1 Nerve experiment

In *Figure 13* is represented the nerve experiment set up. All the recording and stimulating electrodes are immersed in a 0.9% concentration saline solution, which enhances the conductivity of the medium compared to tap water, allowing for better transmission of electrical signals.

From the data acquisition system (DAQ) a stimulus waveform is generated, replicating the following stimulation protocol:

- Pulse shape: biphasic pulse
- Pulse width: 1 ms
- Pulse amplitude: 1 V
- Max repeat rate: 1 Hz
- Sampling frequency: 40 kHz
- Signal duration: 90 ms
- Recording channel input range: $\pm 1V$
- Recording channel resolution: 16 bits

The recording input range refers to the range of input voltages that can be accurately measured by a data acquisition system like LabChart before any gain adjustment is applied. This range is important for ensuring that the system can effectively capture signals of interest without saturating or clipping. On the other hand, the term "16-bit" refers to the resolution of the analog-to-digital converter (ADC) in the PowerLab data acquisition hardware. A 16-bit ADC can represent analog signals with 2^{16} or 65,536 discrete levels, providing high-resolution digitisation of the input voltage range. So, while the recording input range defines the span of voltages that can be measured before any amplification or attenuation, the 16-bit resolution of the PowerLab ADC ensures precise digitisation of these voltage levels, enabling accurate representation and analysis of recorded data.

The stimulus signal (in volts) goes through the isolation unit (model 2200, AM-Systems, USA), which provide a physical barrier that helps prevent electrical signals from passing directly between the input and output sides and help in minimising electrical noise that may be

present in the system. The isolation unit also converts the voltage signal to a current one (conversion factor 1mA/V). This element is necessary for this experiment because is current based.

Once the stimulus has been delivered via the stimulating electrodes it is detected by the recording electrodes in the saline solution. Using the standard measurement instrumentation, the signal will be amplified (Gain: 1000) and filtered (0.1 Hz low cut off, 20 kHz high cut off) by a bioamplifier (AM-System 1700, U.S. & Canada) and it will be sent to the DAQ (25 kHz low pass filter).

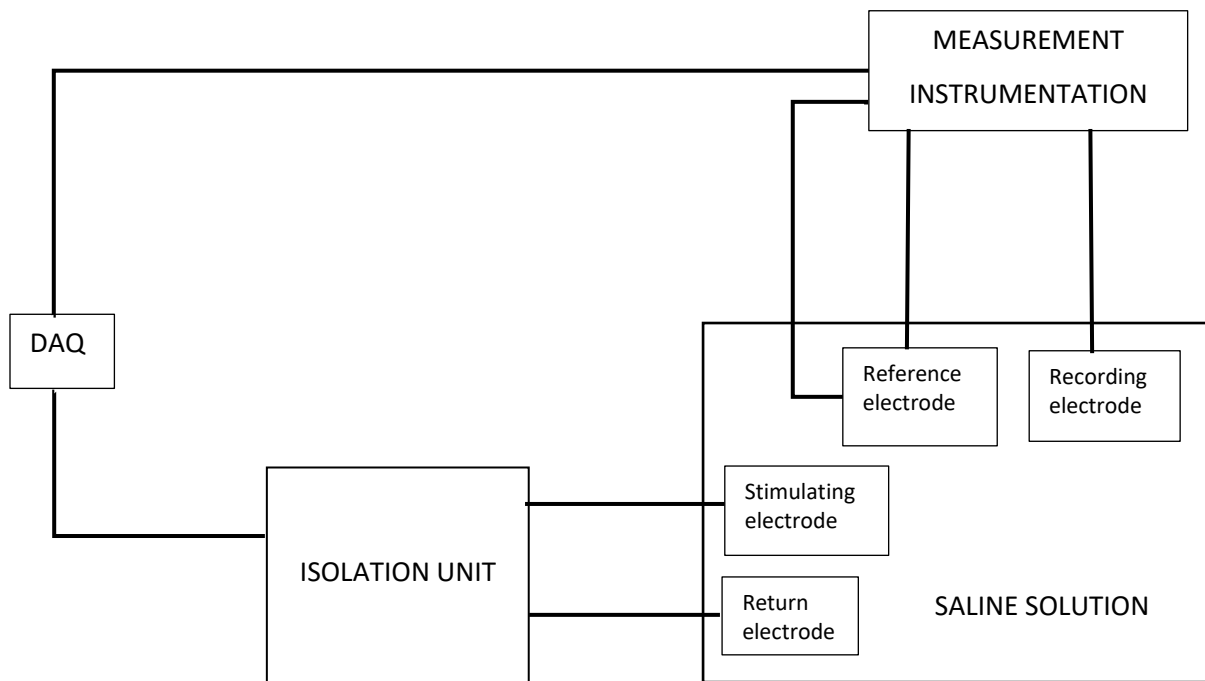


Figure 13 Block diagram nerve experiment set up with standard measurement instrumentation.

Considering the experiment set up with either unpackaged optrode transducer or OpBox, instead of connecting the recording electrode and its reference to the bioamplifier, those must be connected to the optrode's pins or the OpBox's banana socket, as it is represented in Figure 14. Once the recorded signal reaches the optrode then it runs along the path

constructed by the optical fibre and the signal will be converted from optical to electrical by means of the PD. Then, the output electrical signal will enter the DAQ system in order to be further analysed.

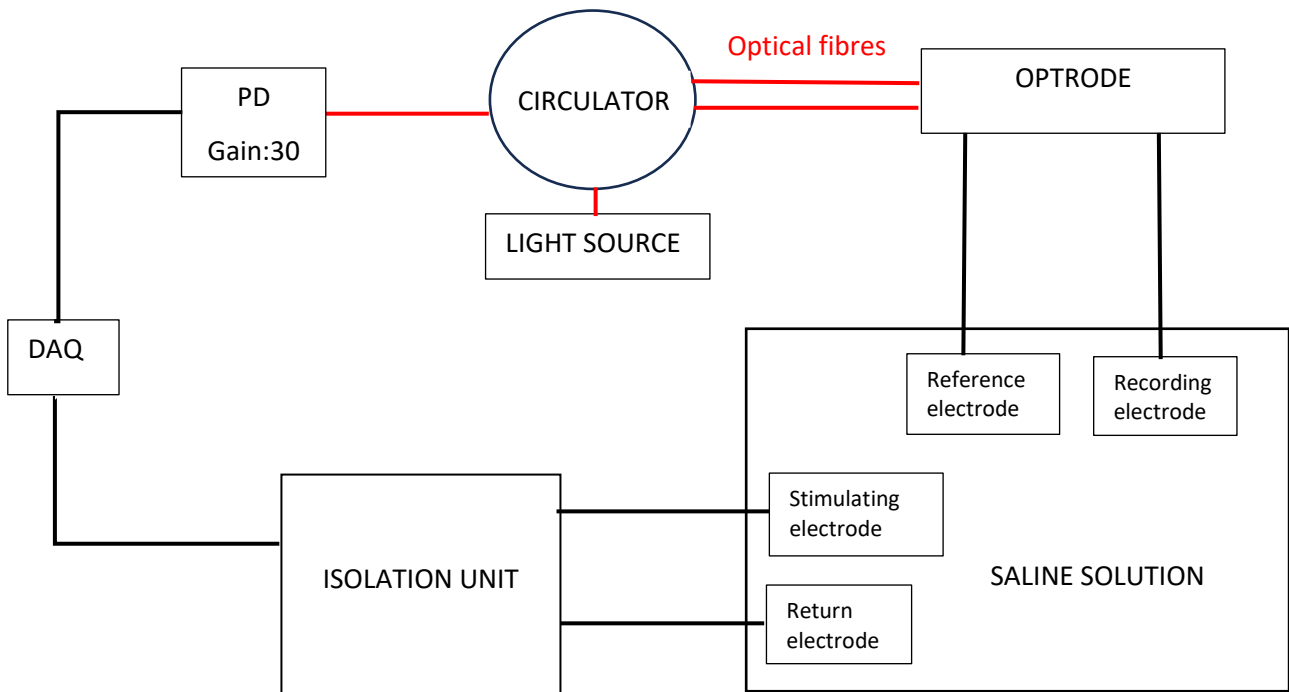


Figure 14 Block diagram experiment set up with optrode. Here the optrode could be either the unpackaged optrode transducer or the OpBox.

4.4.2 Cornea ring experiment

For the cornea ring experiment, a further amplification is necessary to properly detect the signal. In the context of bioelectrodes and bioamplifiers used in biomedical applications, it is often recommended that the input impedance of the amplifier should be much higher than the impedance of the electrode-electrolyte interface.

In the case of the of the considered experiment the input impedance of the AM-System 1700 bioamplifier used for the nerve experiments is too low with respect to the resistance of the cornea ring electrode. If the amplifier impedance is low compared to the electrode impedance, the amplifier can effectively "load" the electrode, affecting the electrode potential and causing distortion of the measured signal. This loading effect can introduce errors and alter the characteristics of the signal being measured.

For this reason, the use of alternate bioamplifier (CardioPhys ECG Electrocardiogram Monitoring System, World Precision Instruments (WPI), USA) with a preamplification (x10) headstage was necessary.

As in the previous experiment all the electrodes are immersed in 0.9% saline solution and the electrical signal follows the paths shown in *Figure 15*. From the data acquisition system (DAQ) a stimulus waveform is generated, replicating the following stimulation protocol:

- Pulse shape: pulse
- Pulse width: 0.5 ms
- Pulse amplitude: 1 V
- Max repeat rate: 1 Hz
- Sampling frequency: 40 kHz
- Signal duration: 1 s
- Recording channel input range: $\pm 1V$
- Recording channel resolution: 16 bits

Once the stimulus has been delivered, it enters the isolation unit, which converts the voltage signal to a current one (conversion factor 1mA/V) and then delivered to the stimulating electrode. Thanks to the conductivity of the medium, the signal will be detected through the

recording electrode and sent to the headstage, fundamental for its role of interface for electrodes with external recording equipment, in this case the bioamplifier CardioPhys ECG Electrocardiogram Monitoring System. The bioamplifier receives the raw electrical signal, remove unwanted frequency components, inserting a low pass filter at 0.1 Hz and a high pass filter at 10 kHz and amplifying (Total gain: 100) the signal to a level that is detectable and measurable by the DAQ.

However, for the corneal ring experiment set up with the optrode, reference can be made to *Figure 14*, since the measurement system circuit it will be the same for all the case studies, what does it change is the type of electrodes that will be used.

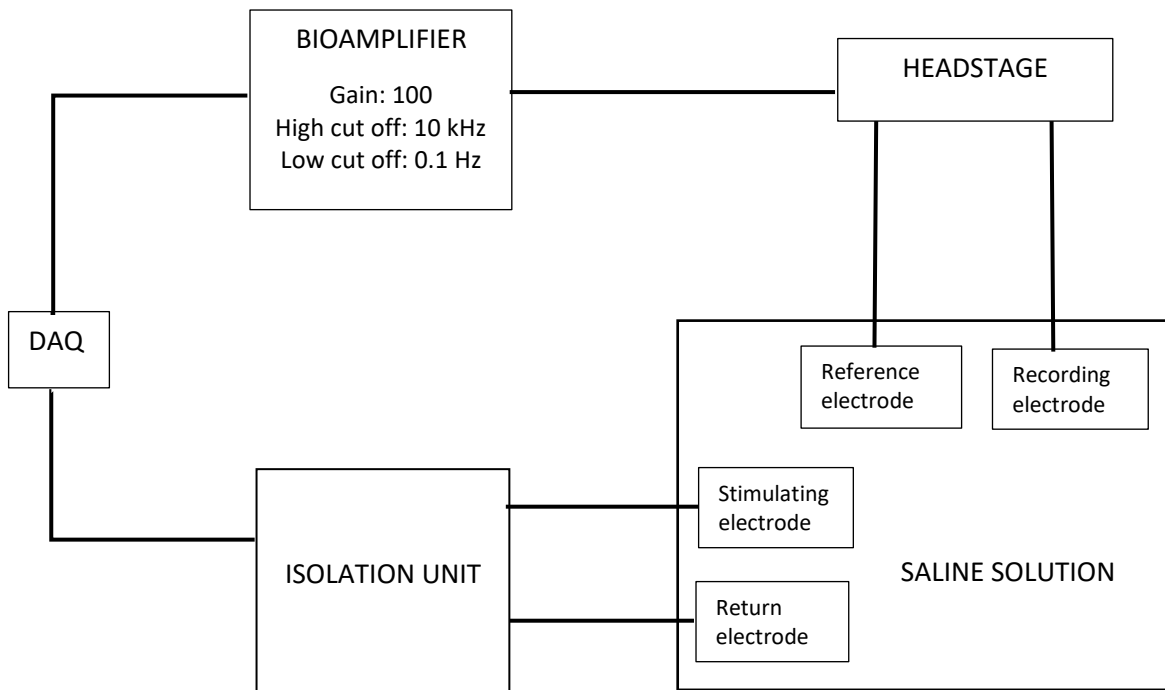


Figure 15 Block diagram of the cornea ring experiment setup with standard measurement instrumentation.

4.4.3 Artificial vision experiment

Regarding the artificial vision experiment a monopolar patch pipette is used as recording electrode; this has to necessarily be plugged into a headstage bioamplifier, in order to acquire the electrical stimulus. *Figure 16* represents the signal pathway. From the DAQ a stimulus waveform is generated, replicating the following stimulation protocol:

- Pulse shape: pulse
- Pulse width: 0.2 ms
- Pulse amplitude: 1 V
- Max repeat rate: 25 Hz – 500 Hz
- Sampling frequency: 100 kHz
- Signal duration: 1 s
- Recording channel input range: $\pm 1V$
- Recording channel resolution: 16 bits

After the stimulus is delivered, it passes into the isolation unit, where it undergoes a conversion from a voltage signal to a current signal at a rate of 1mA per volt. Subsequently, the converted signal is directed to the stimulating electrode. Due to the conductivity of the surrounding medium, the signal is then picked up by the recording electrode and routed to the headstage. The headstage plays a critical role as an intermediary between the electrodes and external recording equipment, facilitating signal amplification and conditioning for accurate transmission. Furthermore, this headstage contains amplifier circuitry that amplifies the signal while minimising noise. After that, the electrical signal enters the standard measurement instrumentation Axon Axoclamp 900a (Molecular device, USA) where the signal will be further amplified (Gain: 1000) and filtered (0.1 Hz low cut off, 20 kHz high cut off). Its output will be then sent to the DAQ for further analysis.

For the experiment set up with the optrode, reference can be made to *Figure 14*, following what stated previously, underlying the simplicity and the functionality of the optrode system.

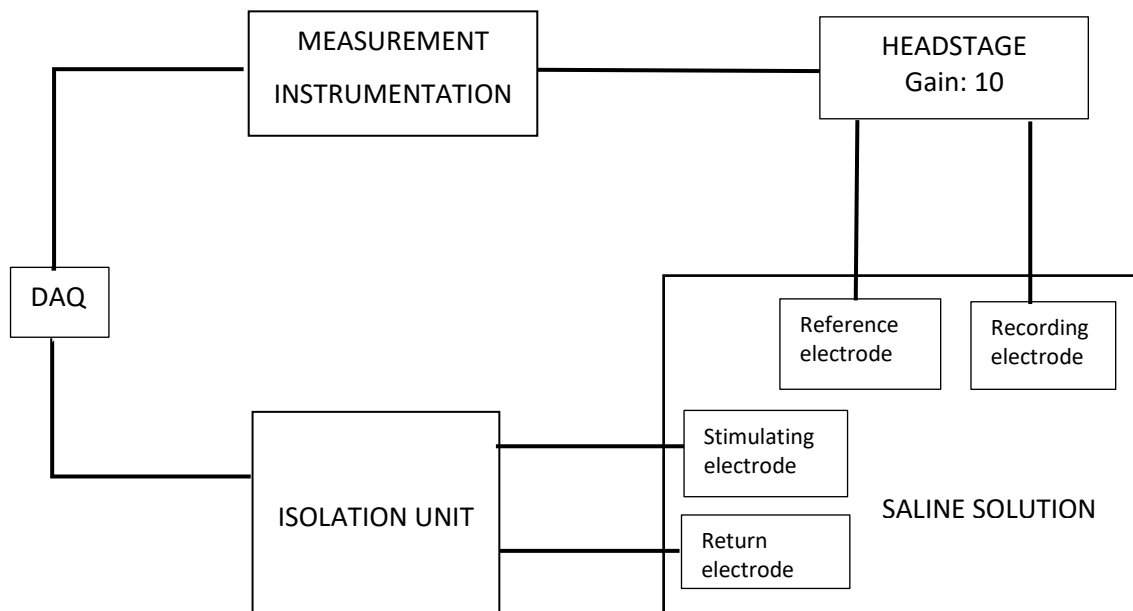


Figure 16 Block diagram of the artificial vision experiment setup with standard measurement instrumentation.

4.4.4 Ex vivo experiment

Investigating stimulation artefacts through *ex vivo* analysis offers several advantages for comprehending the effects of the OpBox and accurately portraying the body's response to stimulation while recording electrophysiological signals, as opposed to simulated laboratory environments. For instance, *ex vivo* experiments utilise intact tissue samples obtained directly from living organisms, preserving the physiological environment and cellular interactions. This maintains the relevance of the experimental findings to *in vivo* conditions and closer to the reality compared to *in vitro* conditions. Furthermore, *ex vivo* experiments could involve the use of tissue samples obtained post-mortem or from animal models euthanised for other purposes, reducing ethical concerns compared to experiments conducted on live animals, and reducing overall numbers of animals used in research. Overall, *ex vivo* analysis for stimulation and recording electrophysiological signals provides a valuable bridge between *in vivo* and *in*

vitro studies, offering a compromise between physiological relevance and experimental control.

The selection of the nerve experiment was deliberate due to its practical application and the ease of electrode placement. Additionally, the nerve experiment exhibited the highest degree of consistency across various experimental conditions. Replicating the experiment initially with the standard measurement instrumentation and then with the OpBox as the recording system involved placing stimulating electrodes on the rat's paws and positioning the recording electrode and its return in the rat's leg cavity to access the nerve. The recording site was soaked with 0.9% saline solution, maintaining tissue hydration, in order to enhance electrical conductivity of the nerve tissue. This allows better transmission of electrical signals, facilitating the detection of stimulation artefacts with greater sensitivity and accuracy.

4.4.5 *In vivo* experiment

Conducting an *in vivo* experiment after an *ex vivo* experiment allows researchers to validate their findings, confirm their relevance to physiological processes, and assess the potential clinical implications of their research in a more comprehensive manner. Additionally, validating the OpBox system *in vivo* on rats provides valuable data that can inform its potential clinical applications. If the system performs well in animal studies, it may pave the way for future translation into human studies and clinical trials

One week before the submission of my report an unplanned opportunity arose to conduct an *in vivo* experiment and test the OpBox I had developed, following presentation of my results to collaborators from the Faculty of Medicine whom I interviewed at the start of the project (Nerve case). This experiment was planned, executed and below is a summary of the results, given the limited time left to conduct in-depth quantitative analysis.

An *in vivo* experiment was conducted on a single rat covered under the ethics approval of Dr Felix Aplin. The rat was sedated using a single injection of urethane. The sciatic nerve from

one hind leg was exposed and kept moist by the addition of paraffin oil. Stimulation electrodes in the form of hypodermic needles were placed on the corresponding paw of the rat. A platinum hook electrode was placed on the sciatic nerve and a ground recording electrode placed in nearby tissue underneath the skin. This allows bipolar electrical stimulation and monopolar recording of evoked responses. The recording electrodes were connected to either a CardioPhys amplifier or the OpBox. Electric pulses were delivered to the stimulating electrodes from a stimulus isolation unit driven by input from the DAQ.

Due to time constraints, a quantitative analysis using MATLAB was not conducted in this experiment. The focus was primarily on the experimental setup, data collection, and initial observations on LabChart. While quantitative analysis using MATLAB could provide valuable insights, its implementation would have required additional time for data processing, analysis, and interpretation. Therefore, the decision was made to defer the quantitative analysis to future experiments or research endeavours. However, inserting the following qualitative analysis, from the LabChart's scope view, still a good tool in order to confirm and validate the OpBox results obtained in the previous experiments.

Various stimulation protocols were examined to assess the presence and effectiveness of the nerve signal. This approach was adopted to ensure that the recorded signals were not merely artefacts but indeed indicative of genuine nerve responses.

4.5 Software

In all the experiments, LabChart (ADInstruments, ANZ), in conjunction with a PowerLab recording unit, is used. It offers versatile data acquisition and analysis solutions. The systems are used together with computers to record and analyse physiological signals from human and animal subjects. In one compact unit, PowerLab systems perform the functions of chart recorders, XYT plotters, digital voltmeters, and storage oscilloscopes. LabChart also supports the export of a file in MATLAB format.

For this project all the signal analysis has been done with MATLAB software, a high-performance language that is used for technical computing. It provides functions to manage, analyse, preprocess, and extract features from uniformly and nonuniformly sampled signals.

Furthermore, to properly analyse all the recorded signal, the subtraction technique has been used to remove the baseline shifts.

Here is how the subtraction technique works:

1. Calculate the mean: compute the mean value of the signal by summing all data points and dividing by the total number of data points. In our case it was calculated the average of just the last 30 ms to estimate the baseline after settling from the delivery of the pulse. Further explanations will be given in section 5.
2. Subtract the mean: subtract the mean value obtained in step 1 from each data point in the signal.

Mathematically, the subtraction technique can be represented as follows:

$$N(t) = S(t) - \mu$$

Where:

- $N(t)$ represents the normalised signal.
- $S(t)$ represents the original signal.
- μ represents the mean value of the original signal

This process centres the signal around zero, effectively removing any constant offset or baseline shift. It can be particularly useful when analysing signals with varying baseline levels or when comparing signals with different baseline characteristics.

After applying the subtraction technique, the resulting signal have a mean value of zero and facilitate further analysis, such as calculating signal features, detecting peaks, or comparing signals across the different experiments and conditions, which will be presented in the following section.

5. Interpretation and Discussion of Results

5.1 Gain measurement

As stated in section 4, to properly investigate if the OpBox could introduce any noise or affect the signal a gain measurement was done. Firstly, considering the optrode transducer by itself and then performing a gain measurement with the optrode packaged inside the EMI shielded box (OpBox).

An understanding of the inverse of the gain, i.e. attenuation, is useful for analysing systems in which gain adjustments or compensation are required. From a quantitative analysis in LabChart, formulae (1) and (2) show how the two measured gains were calculated. The input signal, denoted as V_{in} , represents the voltage applied directly to the optrode. In this scenario, a sinusoidal signal with peak-peak difference voltage of 2V was applied. The output signal, denoted as V_{out} , refers to the voltage measured using the photodetector, which converts the optical signal into an electrical signal. It represents the response or output of the system to the applied input signal. The output signal has a lower amplitude respect to the input signal due to the different attenuation level of the measurement system. In formulae (1.1) and (2.1) the gain adjustment was calculated. From this analysis, it can be stated that the OpBox provides less attenuation of the signal. This can probably be attributed to the reduction of electromagnetic interference. Using only the simple transducer, the signal may be susceptible to interference from external electromagnetic sources present in the environment. Interferences can distort or weaken the signal, leading to higher attenuation. Placing the transducer in an EMI shielded box provides a barrier against external electromagnetic fields. The shielding prevents outside interference from affecting the signal, resulting in clearer and stronger signal transmission with lower attenuation. By minimising electromagnetic interference, the signal maintains its integrity better within the shielded box. In addition to

the preservation of signal quality, a better optical fibres control, a fixing of the transducer in a ring and a better connection to electrodes leads to reduced attenuation as the signal travels through the experimental setup.

Overall, the use of an EMI shielded box helps to create a controlled environment where external electromagnetic interference is minimised, leading to lower attenuation and more reliable experimental results.

$$G1 = \frac{V_{out}}{V_{in}} = \frac{0.11 V}{2 V} = 0.055 \quad (1)$$

$$G1^{-1} = \frac{1}{0.055} = 18 \quad (1.1)$$

$$G2 = \frac{V_{out}}{V_{in}} = \frac{0.1838 V}{2 V} = 0.0919 \quad (2)$$

$$G2^{-1} = \frac{1}{0.0919} = 10 \quad (2.1)$$

Proceeding with the study using MATLAB, a baseline noise analysis of the recorded signal was done. This is essential for ensuring the reliability, accuracy, and performance of the measurement systems, as well as for optimising the experimental conditions. By analysing the noise floor (the level of unwanted signals present when no meaningful signal is present) it is possible to determine how much the measured signal is above the noise, which is essential for accurate data interpretation.

Considering that the input signal is a sine function, an output signal as a sine function with a certain level of noise is obtained. In order to properly analyse the noise level, a notch filter at 1 Hz (the frequency of the applied sine signal) was used, designed to attenuate or eliminate frequencies around the 1 Hz range while allowing other frequencies to pass through relatively unaffected. The baseline portion of the signal is defined based on the entire duration of the signal and considering the centred data, obtained through the subtraction technique, also known as mean normalisation, mentioned in section 4.

Table 2 shows the results:

	Baseline standard deviation (mV)
Unpackaged Optrode	0.315
OpBox	0.3075

Table 2 Unpackaged optrode and OpBox baseline noise standard deviation.

Comparing the baseline standard deviations offers valuable insights into the noise levels inherent in each signal. Generally, higher standard deviations correspond to increased noise levels within the signal. Upon examination, it was found that both the unpackaged optrode and OpBox signals exhibited similar baseline standard deviations, suggesting comparable noise levels between the two. This analysis confirmed that there was no significant difference between the unpackaged optrode and OpBox signals. Consequently, it can be inferred that the OpBox does not introduce any additional noise or distortions into the signal when compared to the optrode.

Further analysis, such as signal-to-noise ratio calculations or visual inspection through the PSD of the signals, may be necessary for a comprehensive comparison. Formula (3) is used to calculate the SNR and Table 3 shows the results. Peak-peak amplitude and baseline standard deviation were measured in volts.

$$SNR = 20 \times \log_{10} \left(\frac{\text{peak - peak amplitude}}{\text{baseline standard deviation}} \right) \quad (3)$$

	SNR (dB)
Optrode	16.031
OpBox	15.5718

Table 3 Unpackaged optrode and OpBox SNR.

A higher SNR generally indicates a better signal quality, as it means the signal's strength is relatively higher compared to the noise level. The SNR results confirm what stated before, notably, the observed values demonstrate a mere 0.5 dB difference between the two conditions. This minimal variance suggests that the signal strength remains consistently higher than the noise level across the examined scenarios.

In addition to the quantitative analysis, a visual comparison of the two different PSDs can be made in *Figure 17*, confirming the above statement. The two graphs do not differ too much from each other, both showing an exponential trend at low frequencies and a flat trend at higher frequencies, providing a consistent noise floor at all frequencies.

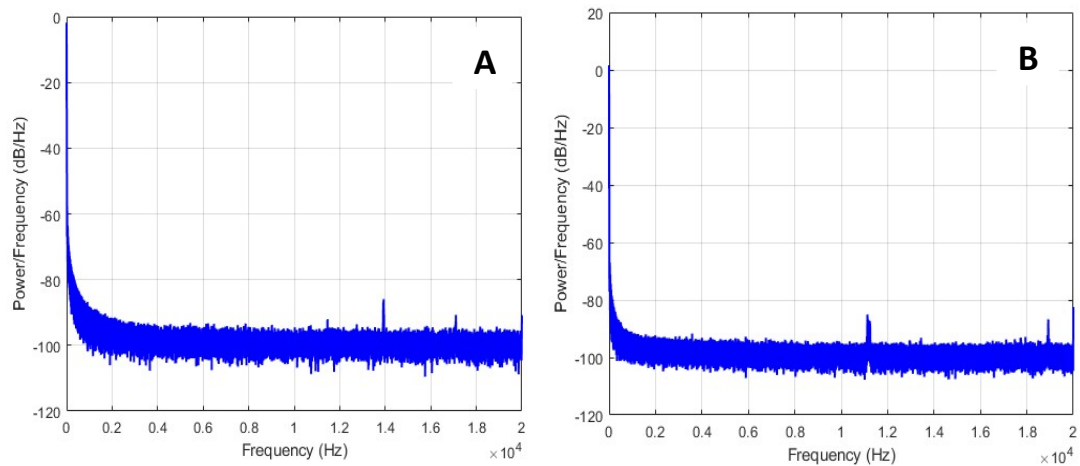


Figure 17 PSD (A) Unpackaged optrode. (B) OpBox

5.2 Case studies

In the following subsections the results obtained for each case study will be presented. This will include an analysis of the standard measurement instrumentation and OpBox performances, in order to highlight their differences. Then a comparison between the unpackaged optrode transducer and the OpBox performance has been done to validate what was stated previously.

5.2.1 Nerve experiment

Delivering the biphasic stimulus pulse with a 30 ms delay because of the initial oscillation observed in the OpBox case is a crucial adjustment in experimental protocol that has been done. This approach likely helps to ensure that the recorded signals are not affected by any transient artefacts or oscillations that may occur immediately after the stimulus onset. The cause of that oscillation is software related to the PowerLab DAQ hardware, which reason why has to be investigated, but it is out of the scope of this project.

Figure 18 reports the results obtained with the standard measurement instrumentation (*Figure 18A*) compared to the one obtained with the OpBox (*Figure 18B*). The similarity in artefact amplitude between the two conditions (around 4mV) suggests that both are capable of capturing similar signal intensities. However, the key advantage of the OpBox, lies in its ability to start and end the artefact noise precisely at the same time as the biphasic stimulus pulse, without any recovery time. This feature is crucial because it ensures that there is no overlap between the artefact and the physiological signal of interest which is expected to occur after the stimulus pulse, reducing the risk of data loss or distortion. By eliminating the need for recovery time, researchers can capture the signal of interest more accurately and efficiently, leading to a clearer understanding of the underlying electrophysiological processes.

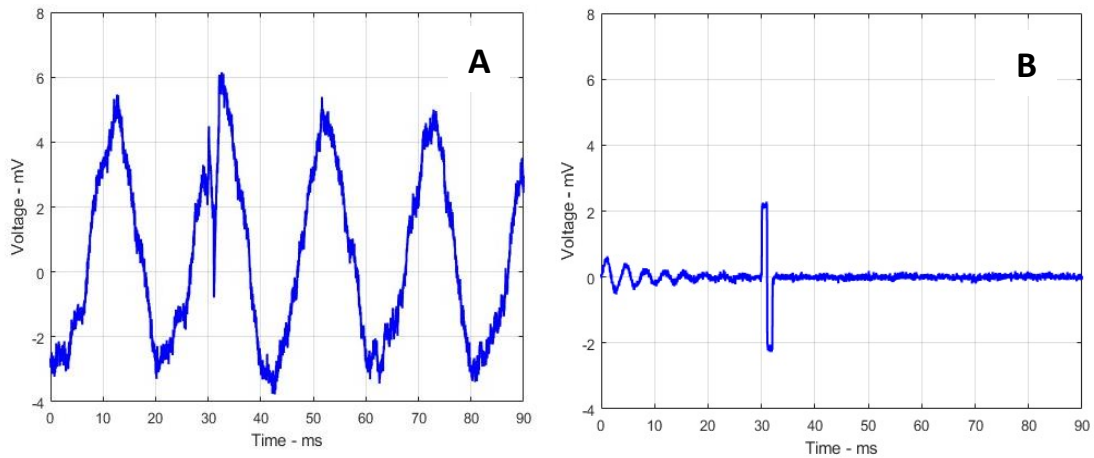


Figure 18 Nerve benchtop experiment. Stimulus artefact measurements in saline. (A) Standard measurement instrumentation. (B) OpBox. Displayed signals are an ensemble average of 100 repeats.

The absence of 50 Hz noise in the signal obtained with the OpBox compared to the evident presence of this noise in the signal from the standard measurement instrumentation is indeed another crucial finding. This difference suggests that the OpBox may inherently suppress or eliminate 50 Hz noise without the need for additional filtering. The presence of 50 Hz noise can be problematic in electrophysiological recordings as it can obscure the signal of interest and introduce artefacts that may interfere with data analysis. The fact that the OpBox captures clean signals without the need for filtering indicates its superior performance in terms of signal clarity and fidelity. This finding not only simplifies experimental setups by eliminating the need for additional noise filtering but also enhances the reliability and accuracy of the recorded data.

As a matter of consistency, a baseline noise analysis based on the control measurement taken with the optrode and with the OpBox has been done. *Figure 19* likely depicts the results of this analysis, showing that the OpBox exhibits some degree of lower isolation compared to the optrode alone. The presence of the EMI shielded box in the OpBox setup is intended to minimise environmental electromagnetic interference, which can otherwise introduce unwanted signals or noise into the measurements.

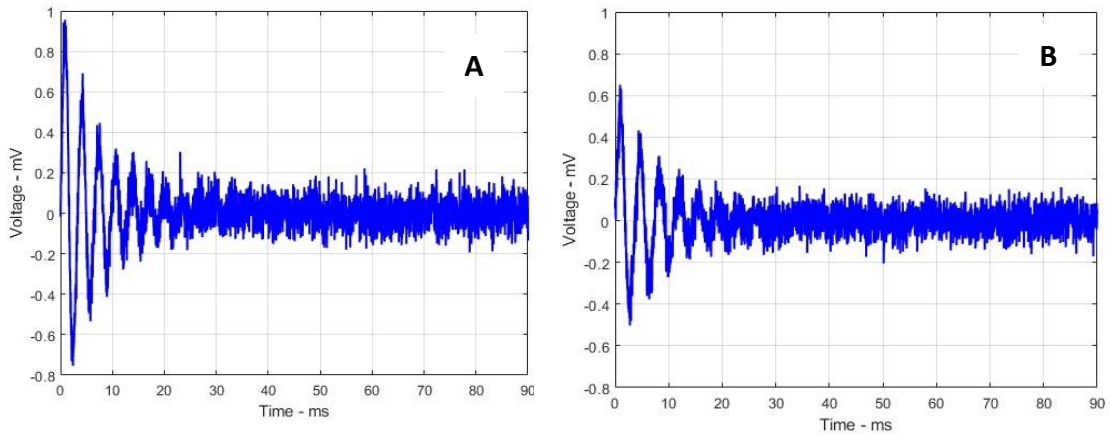


Figure 19 Benchtop experiment using the Nerve case. Control measurements – stimulus set to 0V. (A) Unpackaged optrode. (B) OpBox.

Referring to *Table 4* for a quantitative analysis: calculation of the standard deviation of the baseline noise over the last 30 milliseconds of the signal is a good strategy to mitigate the initial oscillation effect and focus on the stable portion of the data. By averaging over this time window, it was easier to assess the typical level of noise present in the measurements without being influenced by transient effects at the beginning of the recording.

	Baseline standard deviation (mV)
Bioamplifier instrumentation	0.819
Unpackaged Optrode	0.385
OpBox	0.268

Table 4 Baseline analysis nerve experiment.

From these results, it can be stated that the OpBox setup exhibits lower baseline mean and standard deviation values compared to the optrode setup. This suggests that the OpBox enclosure is effective in reducing baseline noise, as evidenced by the lower standard deviation value. This quantitative analysis validates the qualitative observations made earlier and underscores the benefits of using the OpBox enclosure for minimising electromagnetic interference and improving signal quality in optrode measurements. For the sake of consistency, we have included the standard measurement instrumentation baseline standard deviation, despite its inherent high noise level deriving from 50 Hz interference.

5.2.2 Cornea ring experiment

Figure 20 illustrates the complete signal acquisition process for both the bioamplifier and OpBox setups, with the pulse stimulus administered after a 30 ms delay. Despite employing a notch filter in the bioamplifier setup, the persistent presence of 50 Hz noise remains noticeable. In contrast, the OpBox configuration operates effectively without the necessity for supplementary filtering adjustments and significantly reduces the amplitude of the 50 Hz oscillations. Additionally, the OpBox configuration demonstrates a reduced artefact amplitude in comparison to the bioamplifier configuration, indicating superior performance in terms of signal fidelity and interference mitigation. These findings underscore advantages of the OpBox, which delivers enhanced noise reduction and artefact suppression without the requirement for additional filtering adjustments.

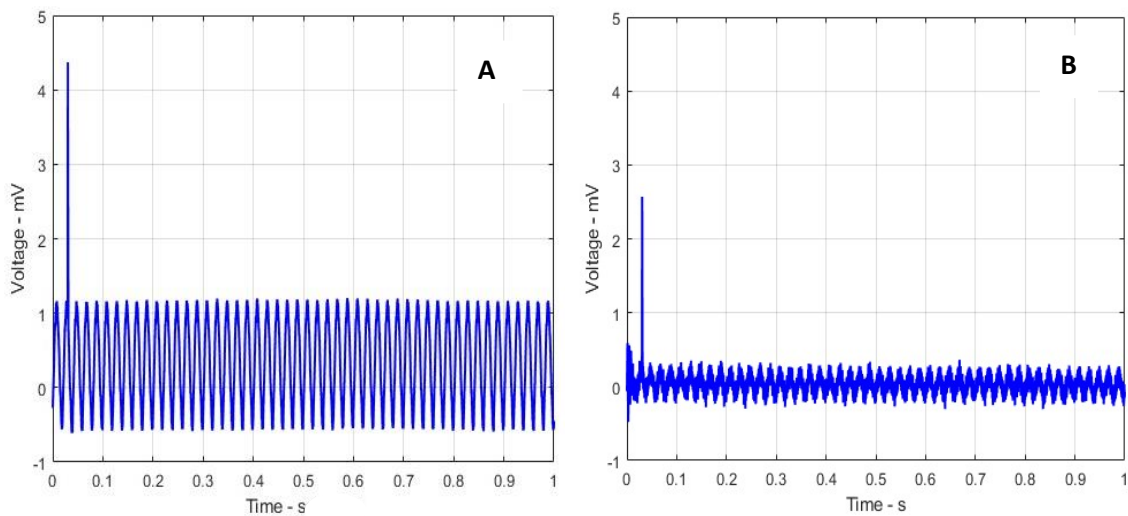


Figure 20 Cornea benchtop experiment. Stimulus artefact measurements in saline(A) Standard measurement instrumentation. (B) OpBox. Displayed signals are an ensemble average of 100 repeats.

In *Figure 21*, a close-up examination of the signal artefacts is provided, particularly focusing on their emergence following the pulse delivery at 0.03 seconds. This zoomed-in view offers

enhanced clarity for analysing the responses of these artefacts and provides valuable insights into their characteristics. In *Figure 21B*, the initial oscillation remains discernible, however, the amplitude of the artefacts is notably reduced compared to *Figure 21A*. This observation validates the findings presented in *Figure 20*, highlighting the superior performance of the OpBox in minimising artefacts.

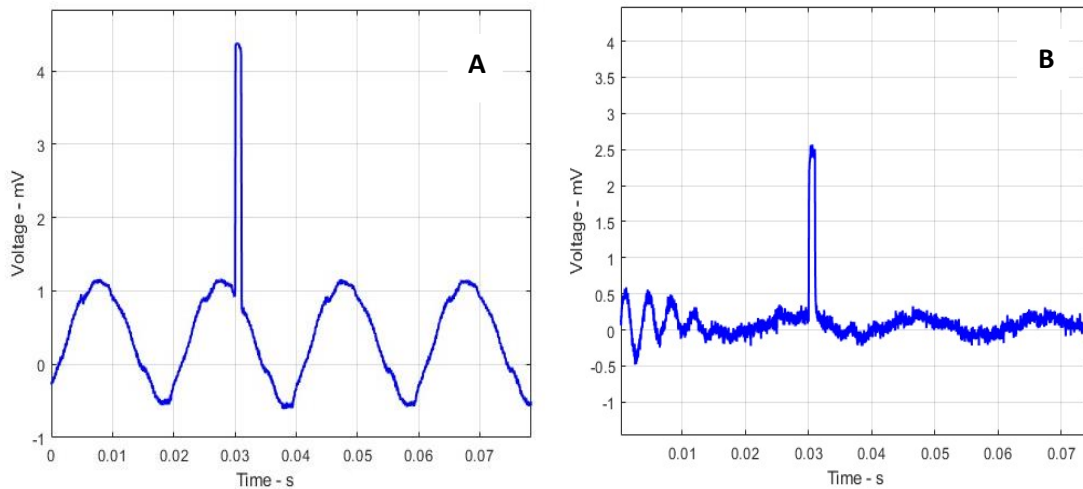


Figure 21 Zoomed- in view cornea benchtop experiment. Stimulus artefact measurements in saline (A) Standard measurement instrumentation. (B) OpBox. Displayed signals are an ensemble average of 100 repeats.

Comparing optrode and OpBox performances, *Figure 22* presents the control measurements of both cases (i.e. when the stimulus pulse amplitude was set to 0 mA), accompanied by the findings summarised in *Table 5*. The data reaffirms that the OpBox setup preserves the signal integrity without introducing any distortion. Quantitatively, the values obtained from both setups are comparable, indicating no significant statistical difference. It is worth noting that some variability may influence the experiment due to slight differences in electrode positioning. However, efforts have been made to replicate the two experiments as closely as possible, ensuring a fair comparison.

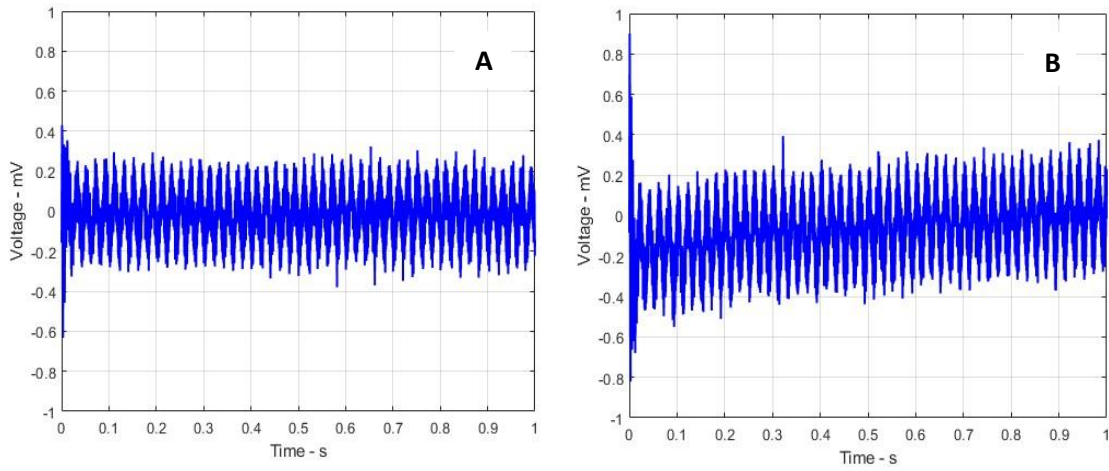


Figure 22 Benchtop experiment using the cornea ring case. Control measurements – stimulus set to 0V. (A) Unpackaged optrode. (B) OpBox.

	Baseline standard deviation (mV)
Bioamplifier instrumentation	0.748
Unpacked Optrode	0.252
OpBox	0.218

Table 5 Baseline analysis cornea ring experiment.

In Table 5 still noticeable the high noise level deriving from 50 Hz interference in the standard measurement instrumentation case.

5.2.3 Artificial vision experiment

When attempting to replicate an experiment using patch pipette recording electrodes, several challenges and disadvantages may arise. For instance, each patch pipette electrode is unique, with variations in tip size, resistance, and surface properties. Even if the same electrode manufacturing protocol is followed, subtle differences in fabrication can lead to variability in recording quality between experiments. Furthermore, manipulating patch pipette electrodes requires precision and skill. Variability in electrode handling, such as pipette positioning, angle of approach, and contact pressure, can affect recording quality. More in general, the physical shape or characteristics of the artefact being measured are influenced significantly by how the electrodes are positioned. Due to the sensitivity of the artefact's shape to electrode positioning, variations in the placement of electrodes would likely lead to differences in the measurements obtained. In other words, small changes in electrode positioning could result in noticeable differences in the data collected during measurements. Consistent electrode positioning is necessary to ensure the repeatability and reproducibility of experimental results. If electrodes are not placed consistently across experiments or subjects, it becomes challenging to compare data sets reliably. Inconsistent positioning can introduce variability into the data, making it difficult to draw valid conclusions or identify meaningful patterns, thus leading to misinterpretation of results or erroneous conclusions about the underlying phenomena being studied.

Overall, for the reasons stated above the “Artificial vision experiment” could not be considered for an accurate comparison between the simple optrode and the OpBox, due to the difficulty of maintaining the same electrode positioning between the two different experiments set up, both with the bio-amplifier, the optrode and the OpBox. For further clarification, please refer to Appendix B.

5.3 *Ex vivo* Nerve experiment

In the final stage of our series of experiments, the *ex vivo* post-mortem nerve experiment was conducted. In this specific experiment, a focus has been made on comparing the performances of the standard measurement instrumentation and the OpBox. The decision to exclude the unpacked optrode from this comparison was made based on our earlier findings, which confirmed the comparable performances and, in some cases, a better performance of the OpBox over the simple optrode. By narrowing our focus to the standard measurement instrumentation and OpBox setups, we aimed to gain deeper insights into their respective capabilities and limitations in the context of the *ex vivo* nerve experiment.

Different iterations have been done, with different positioning of the stimulating electrode with respect to the recording electrode position. The following results refers to the worst-case scenario that has been obtained, registered when positioning the stimulating electrode as much as close as possible to the hook electrode and in the muscles of the hind leg of the rat, rather than its paw.

In *Figure 23*, a comparison is made between the performances of the standard measurement instrumentation and the OpBox in terms of artefact response.

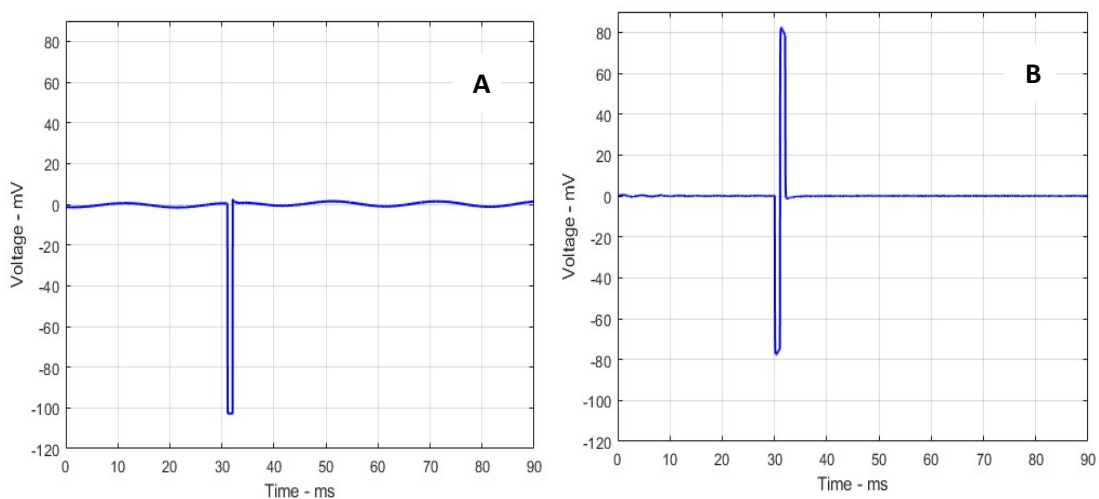


Figure 23 Ex vivo nerve benchtop experiment. Stimulus artefact measurements in saline (A) Standard measurement instrumentation. (B) OpBox. Displayed signals are an ensemble average of 100 repeats.

From *Figure 23A*, the standard measurement instrumentation recording, it is possible to see that one phase is missing, and the peak might reach the limit of the input range of the DAQ, causing it to be cut off during sampling, indicating saturation of either the DAQ or the measurement instrumentation itself. It is worth noting that the OpBox signal (*Figure 23B*) does not saturate. Thus, highlight the advantages of the optrode in terms of not causing saturation of measurement instrumentation, in contrast to the standard measurement instrumentation. This represents a significant hardware advantage, particularly in eliminating stimulation artefacts. The ability of the optrode to avoid saturation ensures that the recorded signals are not distorted or truncated, leading to more accurate and reliable data acquisition. This aspect underscores the superiority of the optrode technology in preserving signal integrity, especially in experiments where high-amplitude signals are expected or when precise measurements are crucial.

While their amplitudes are comparable, *Figure 24* offers a more detailed perspective with a zoomed-in view of the signal response under the two conditions.

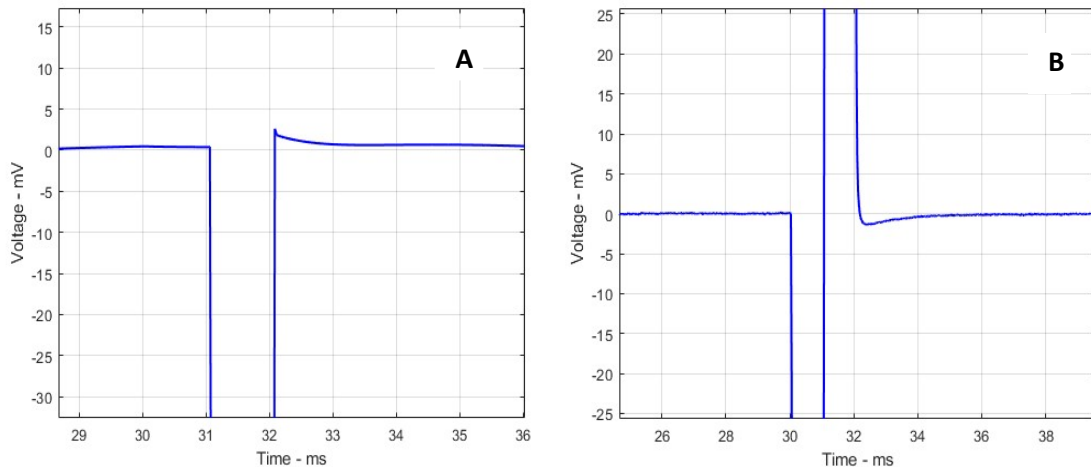


Figure 24 Zoomed- in view *ex vivo* nerve benchtop experiment. Stimulus artefact measurements in saline (A) Standard measurement instrumentation. (B) OpBox. Displayed signals are an ensemble average of 100 repeats.

What is particularly noteworthy in *Figure 24A*, the bio-amplifier case, is the visualisation of an exponential decay. The exponential decay may distort the original signal waveform, making it difficult to accurately interpret or analyse the underlying physiological events. This

distortion can affect the fidelity of the recorded data and may lead to erroneous conclusions. Furthermore, the exponential decay may overlap with or obscuring subsequent signals of interest. This can complicate signal identification and segmentation, making it challenging to isolate specific events for analysis.

In contrast to the standard case, the OpBox signal (*Figure 24B*) consistently demonstrates a lack of significant recovery time, as observed in all experiments. This characteristic facilitates more efficient and accurate signal analysis by eliminating the need to account for prolonged decay periods. The absence of a significant recovery time in the OpBox setup underscores its advantage in providing reliable and high-quality signal recordings, enhancing the overall efficiency and effectiveness of experimental investigations. However, in the OpBox signal, there is a limited exponential rise, after the artefact stimulus, which should not impact the signal processing.

5.4 *In vivo* Nerve experiment

As done in section 4 various stimulation protocols will be presented and discussed together with their results.

Through this approach, a stimulation threshold of 0.75mA pulse amplitude (biphasic) was identified. This threshold signifies that nerve responses were detected when the stimulation pulse amplitude exceeded 0.75mA, whereas below this threshold, only artefacts were observed.

Figure 25 refers to the following stimulation protocol:

- Pulse shape: biphasic
- Phase width: 1ms
- Pulse amplitude: 1mA
- Sampling rate: 40kHz

Figure 26 represents the nerve response set with the following stimulation protocol:

- Pulse shape: biphasic
- Phase width: 1ms
- Pulse amplitude: 0.5mA
- Sampling rate: 40kHz

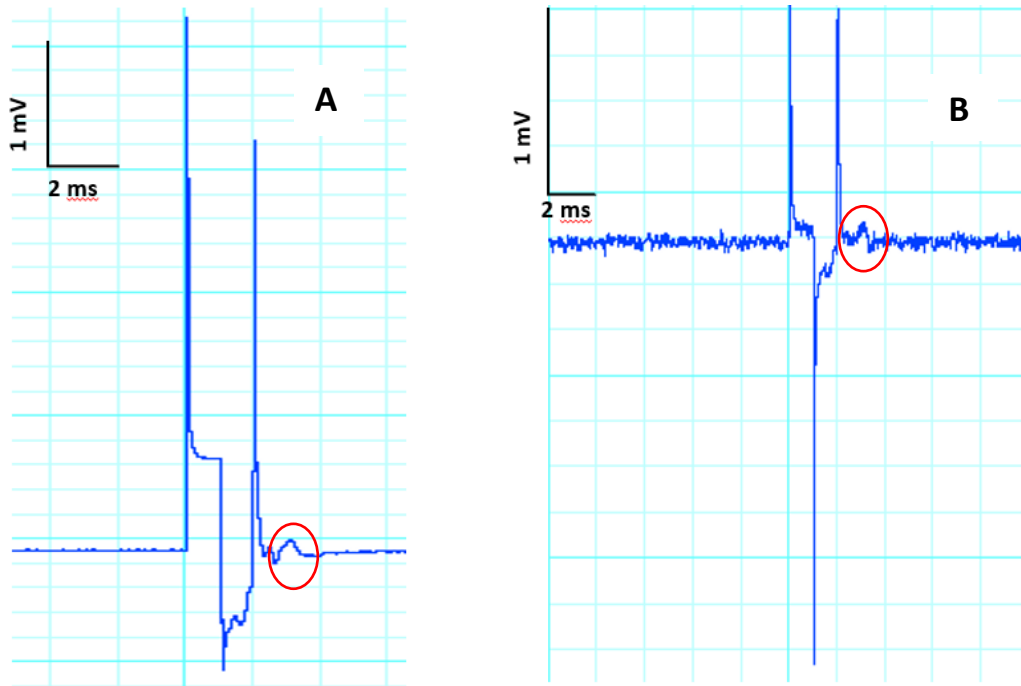


Figure 25 *In vivo* sciatic nerve experiment. Measured responses to a 1 mA, 1ms biphasic stimulus in a rat. (A) Standard measurement instrumentation. (B) OpBox. Displayed signals are ensemble average of 100 repeats. Nerve response highlighted in red circle.

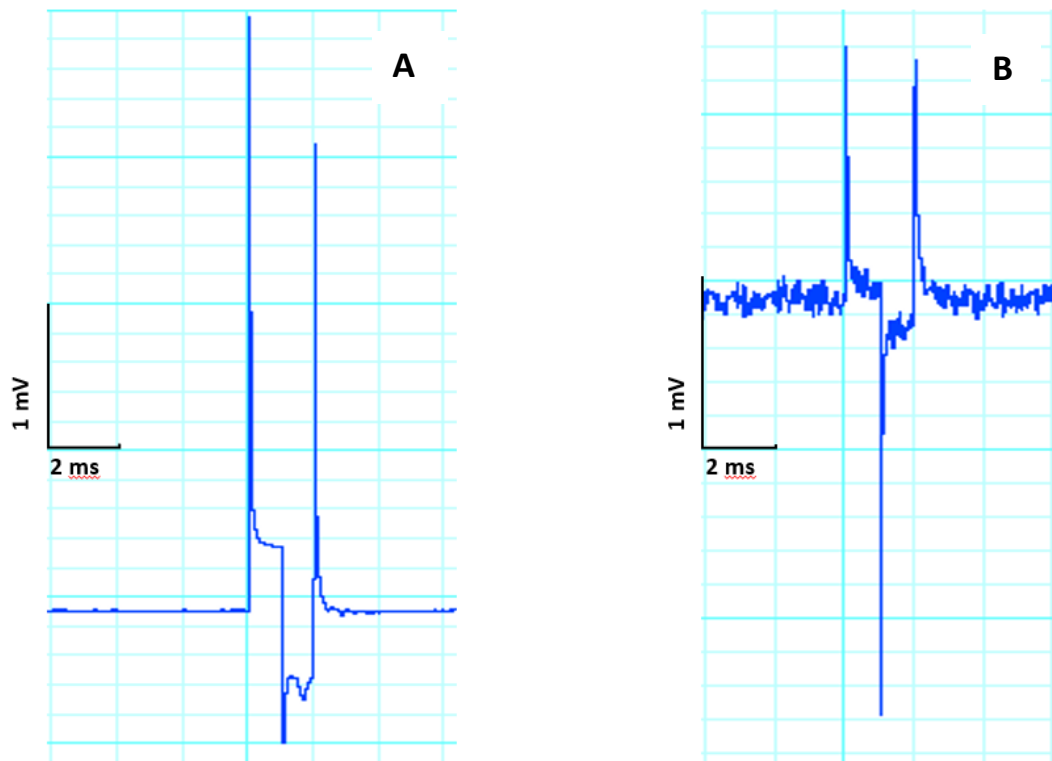


Figure 26 In vivo sciatic nerve experiment. Measured responses to a 0.5 mA, 1ms biphasic in a rat. (A) Standard measurement instrumentation. (B) OpBox. Displayed signals are ensemble average of 100 repeats.

The nerve response can be properly visualised from *Figure 25*, where a stimulus of 1 mA (above threshold) was delivered. *Table 6*, corresponding to *Figure 25*, provides a qualitative assessment of the peak-to-peak difference of the stimulus and its duration. The reported values are adjusted based on the gain of the two different system.

	Peak-peak amplitude (mV)	Duration (ms)
Standard measurement instrumentation	5.3	2.5
OpBox	7	2

Table 6 Artefact analysis for the 1 mA, 1ms biphasic pulse stimulus case.

Despite the slightly lower peak-to-peak amplitude in the standard measurement instrumentation case compared to the OpBox case, it is crucial to observe the duration of the

artefacts. In the standard measurement case (*Figure 25A*), the artefacts exceed the 2 ms biphasic pulse duration, leading to uncertainty and difficulties in interpreting the nerve response. The prolonged artefacts may overlap with the nerve response, hindering a clear analysis.

The presence of a small peak between the artefact and the response could pose a significant challenge for neuroscientists, as it creates uncertainty regarding whether it stems from amplifier ringing or represents an actual neural response. However, in the case of the OpBox (*Figure 25B*), this peak is absent, providing clearer and more reliable data for analysis.

Figure 26, corresponding to the data reported in *Table 7*, reaffirms the earlier observations. In this instance, no nerve response is expected to be visualised as the stimulus delivered is below the threshold. However, in the standard measurement case (*Figure 26A*), an amplifier ringing is apparent. Conversely, in the OpBox case, the stimulus artefact ends precisely when the stimulus pulse concludes.

Regarding the peak-to-peak difference, in the OpBox case, it is slightly lower than in the standard measurement instrumentation case. This observation further affirms its capability to maintain low artefact amplitudes.

	Peak-peak amplitude (mV)	Duration (ms)
Standard measurement instrumentation	5	2.5
OpBox	4	2

Table 7 Artefact analysis for the 0.5 mA, 1ms biphasic stimulus case.

In order to better visualise the nerve response, a faster stimulus (200 μ s) has been delivered. *Figure 27* represents the artefact and nerve response of the following stimulation protocol:

- Pulse shape: biphasic
- Phase width: 200 μ s
- Pulse amplitude: 1.5mA
- Sampling rate: 40kHz

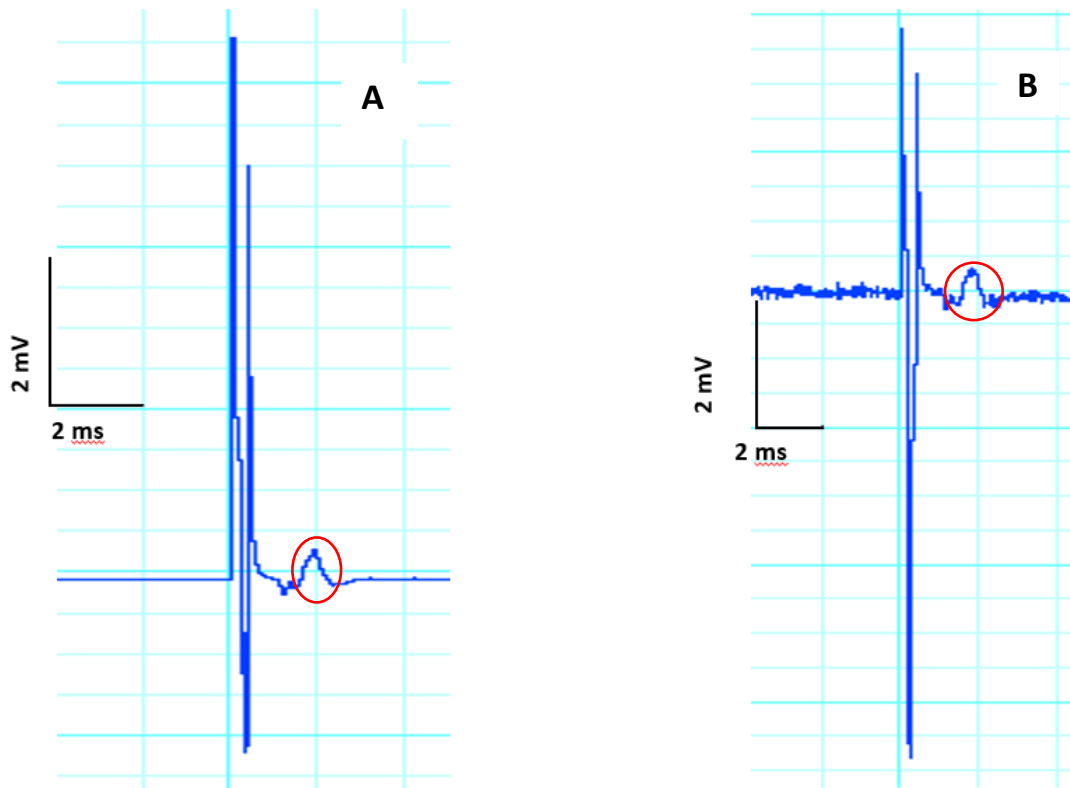


Figure 27 In vivo sciatic nerve experiment. Measured responses to a 1.5 mA, 200 μ s biphasic stimulus pulse in a rat. (A) Standard measurement instrumentation. (B) OpBox. Displayed signals are ensemble average of 100 repeats. Nerve response highlighted in red circle

Table 8, corresponding to Figure 27, reports the qualitative data analysis.

	Peak-peak amplitude (mV)	Duration (ms)
Standard measurement instrumentation	8.4	1.7
OpBox	10.5	0.2

Table 8 Artefact analysis for the 1.5 mA, 200 μ s biphasic stimulus case.

Even in the case of faster stimulus, from Figure 27B highlights the Optrode's rapid response time, ending precisely with the stimulus. Instead, in the standard measurement case (Figure 27A) a peak response is visible before the nerve response, misleading the data processing.

In conclusion, to provide a fair comparison, a recording in response to a biphasic pulse amplitude of 0.5 mA (above the threshold) and a phase width of 200 μ s was conducted. *Figure 28* and the corresponding *Table 9* validate all the previous observations.

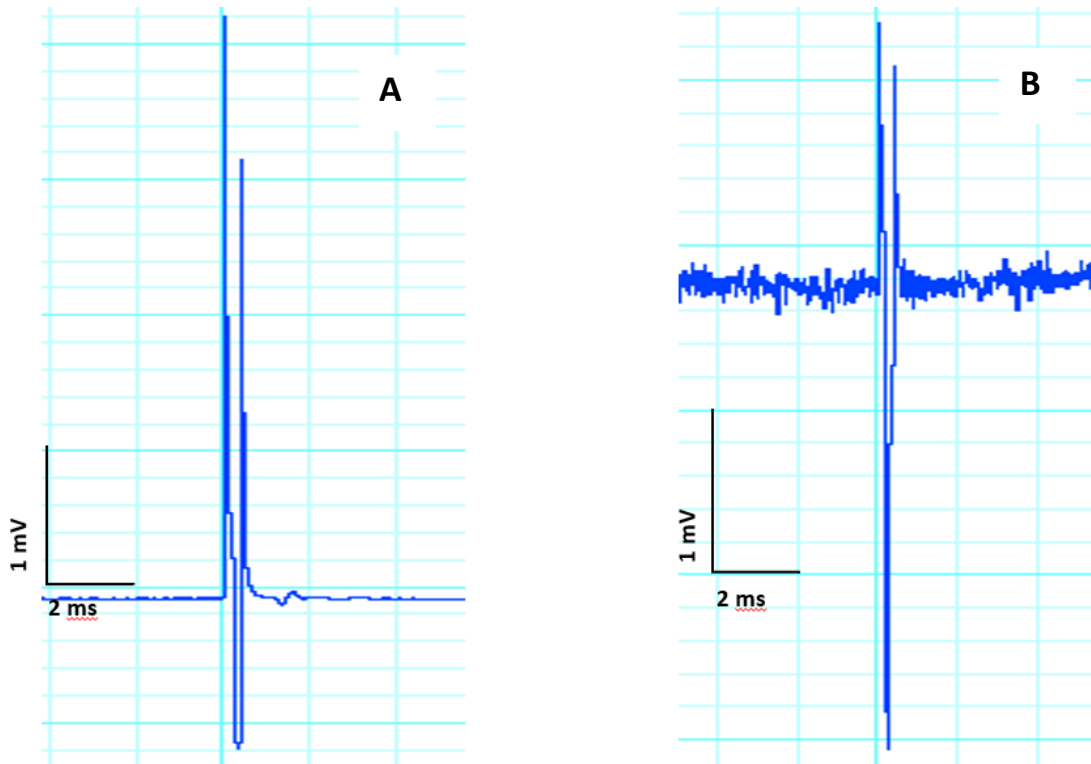


Figure 28 In vivo sciatic nerve experiment. Measured responses to a 0.5 mA, 200 μ s biphasic stimulus pulses in a rat.
 (A) Standard measurement instrumentation. (B) OpBox. Displayed signals are ensemble average of 100 repeats.

	Peak-peak amplitude (mV)	Duration (ms)
Standard measurement instrumentation	5.4	2
OpBox	4	0.2

Table 9 Artefact analysis for the 0.5 mA, 200 μ s biphasic stimulus case.

Figure 28A distinctly demonstrates the presence of prolonged artefact responses, which may overlap with the nerve response if in the case of a stimulus amplitude high enough to evoke

a nerve response. Conversely, *Figure 28B*, in line with previous observations, illustrates the rapid response of the OpBox system and comparable artefact amplitude with the standard measurement instrumentation, without any ringing artefacts that are present in the standard instrumentation case.

6. Conclusions and future developments

The research encompassed in this work spans for a novel optical electrode. Its working principle was discussed in detail, demonstrating the new sensor packaging design as well as the considerations needed for the success of the device. In this report has been proved the ability of one optrode transducer to be a universal 'headstage,' to work with electrodes of various types, together with improvements in minimising artefacts, and relative sensibility to environmental factor have been achieved.

In conclusion, this study presents a comparison between the bioamplifier and OpBox setups in electrophysiological experiments, revealing distinct advantages and disadvantages associated with each recording method. While the bioamplifier setup exhibits noticeable artefacts and prolonged recovery times, the OpBox configuration offers cleaner recordings with minimal recovery time. In this way, researchers can capture the signal of interest more accurately and efficiently, leading to a clearer understanding of the underlying electrophysiological processes. Overall, this discovery together with the ability to plug in any electrode type to the OpBox, represents a significant advancement in the field of electrophysiology, researchers can focus on the underlying physiological events with greater confidence, functionality, leading to improved data interpretation and experimental outcomes.

Moreover, it has been successfully demonstrated the absence of significant 50 Hz noise contamination in the OpBox recordings enhancing the reliability and robustness of data analysis. However, from the analysis is still some residual noise present, possibly due to factors like imperfect shielding or other sources of interference. It might be worth investigating further to determine the specific sources of this lower isolation effect in the OpBox setup and consider any adjustments or additional measures to mitigate it. The work conducted at UNSW, allowed to improve some of the main important features of bio-medical sensors, such as accuracy, resolution, and response time. From the benchtop characterisation of the response of the optical recording system reported, it should be highlighted, that the ability of the device to be both accurate and comparable in terms of response with standard

measurement instrumentation mainly depends on others factor than the transducer itself, such as the positioning of the electrodes.

To summarise, in this thesis, I played a central role in characterising and refining the optrode device, tackling crucial challenges like minimising stimulation artefacts and enhancing device packaging. Through extensive experimental work, I conducted thorough electrical and optical analyses of the sensor, employing benchtop assessments and refining software for precise measurements. Conducting an *in vivo* experiment not only enabled me to further assess the reliability of my previous findings but also paved the way for future development in the field. The implications of my results and enhancements are substantial for the ongoing advancement of optrode neurotechnology.

While the project is advancing, there remains considerable future work to optimise various aspects in the long term. Analysis involving different values of photodetector gain, stimulation current, and temperature must be conducted to further explore the optimal setup resulting in minimal artefact stimulus and a less noisy system. This comprehensive investigation will be crucial for refining the device's performance and enhancing its effectiveness in biomedical applications.

Regarding the OpBox design, improvements should be done in terms of the dimensions to make it more suitable to the biomedical field. Indeed, if the intended use is for *in vivo* brain-machine interfaces, then major effort should be put into making such a design both biocompatible and flexible. Biocompatibility would ensure that the device can be inserted in the body without causing any type of body rejection, such as scar tissue formation or infections, for the safety of the subject implanted as well as long-term reproducible recordings. However, the created functional prototype, stands as one of the initial products slated for commercialisation by Sevren, the startup affiliated with our research group at UNSW.

Finally, another feature which could be added would be to use such device not only for recordings, but also for stimulation. Introducing stimulation capabilities to the device could indeed greatly expand its potential applications in the biomedical field. With such functionality, researchers and clinicians could explore not only recording neural activity but also modulating it, opening doors to therapies and treatments for various neurological

conditions. For instance, in neural interfacing, the ability to stimulate specific neural circuits could aid in understanding brain function and potentially treat disorders like epilepsy or Parkinson's disease. Moreover, bidirectional control of neuro-prosthetics could enable more seamless integration of artificial limbs or sensory devices with the nervous system, improving their functionality and user experience. Implementing stimulation features would require careful consideration of safety, precision, and ethical implications. But with proper development and regulation, it could indeed revolutionise biomedical technologies and enhance the quality of life for many individuals [35].

Appendix A

- Technical datasheet of part components:

Part	Supplier	Link
Optical connector	RS Pro	https://au.rs-online.com/web/p/fibre-optic-adapters/1672842?cm_mmc=AU-PPC-DS3A-_-google-_-PLA_AU_Pmax_FTP_0623-_-_-&matchtype=&&gad=1&gclid=CjwKCAjw7oeqBhBwEiwALyHLM1OaHbQ-CV6R0Ydv1Lq3ek9I23I6rdfOGKZdwCn9jyZFGzSiQhUAlhoCxCMQAvD_BwE&gclsrc=aw.ds
Thorlab ring	THORLABS	https://www.thorlabs.com/thorproduct.cfm?partnumber=C05RC
Banana plug	Staubli	https://au.rs-online.com/web/p/banana-connectors/2615339
Female socket	HIRSCHMANN	https://au.rs-online.com/web/p/banana-connectors/7872962

- Characterisation report transducer TPM-I311-20080005:

Temperature (°C)	24
Humidity (%)	40
S-value (%/V)	18.4
Reflectance at 0 V (%)	4.26
THD at 0.5 V _p (dB)	-31.4
Linearity at 0.5 V _p (%)	2.18
Bandwidth (Hz)	10520
Phase shift at 10 Hz (deg)	-0.097

Table 10 LCs characteristics

Note that by linearity, means non-linearity. Hence the LCs has 2.18% of non-linearity and 9.82 % of linearity.

Appendix B

Figure 29 illustrates the challenge of consistently repositioning the recording electrode (the patch pipette) between the standard measurement instrumentation setup and the OpBox setup. In the standard measurement instrumentation setup, the patch pipette needs to be inserted into the headstage preamplifier. On the contrary, in the OpBox setup, the patch pipette needs to be connected and plugged into the OpBox electrodes interface. Therefore, when removing the patch pipette from the headstage, it necessitates movement.

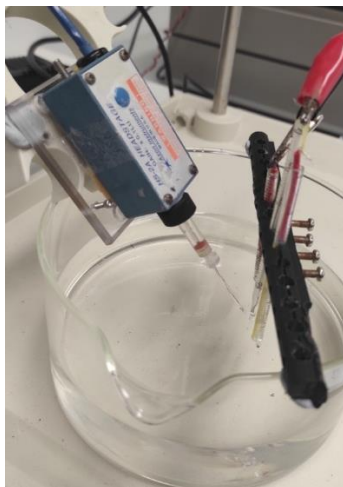


Figure 29 Artificial vision benchtop. Standard measurement instrumentation.

References

- [1] H. N. Rubaiy, "A Short Guide to Electrophysiology and Ion Channels," 2017.
- [2] M. A. Lebedev and M. A. L. Nicolelis, "Brain-machine interfaces: from basic science to neuroprostheses and neurorehabilitation," *Physiol Rev*, vol. 97, 2017.
- [3] C. Clément, *Brain-Computer interface technologies: Accelerating neuro-technology for human benefit*. Springer International Publishing, 2019.
- [4] A. Schousboe, "Advances in Neurobiology Volume 22 Series Editor." 2019.
- [5] M. Ferguson, D. Sharma, D. Ross, and F. Zhao, "A Critical Review of Microelectrode Arrays and Strategies for Improving Neural Interfaces," *Advanced Healthcare Materials*, vol. 8, no. 19. Wiley-VCH Verlag, 2019.
- [6] H. Xiong and H. E. Gendelman, "Current Laboratory Methods in Neuroscience Research." 2017.
- [7] *Basic Electrophysiological Methods (DRAFT)*. Oxford University Press, 2015.
- [8] M. Cerf *et al.*, "On-line, voluntary control of human temporal lobe neurons," *Nature*, vol. 467, no. 7319, 2010.
- [9] M. M. Heinricher, "Principles of Extracellular Single-Unit Recording Extracellular Recording: Neuronal Activity in a Functional Context." 2017.
- [10] J. M. Walker, "Methods in molecular biology tm Series Editor." 2018.
- [11] J. J. Shih, D. J. Krusienski, and J. R. Wolpaw, "Brain-computer interfaces in medicine," *Mayo Clinic Proceedings*, vol. 87, no. 3. Elsevier Ltd, 2012.
- [12] A. Al Abed, H. Srinivas, J. Firth, F. Ladouceur, N. H. Lovell, and L. Silvestri, "A biopotential optrode array: operation principles and simulations," *Sci Rep*, vol. 8, no. 1, 2018.
- [13] J. R. Buitengeweg, W. L. C. Rutten, and E. Marani, "Geometry-based finite-element modeling of the electrical contact between a cultured neuron and a microelectrode," *IEEE Trans Biomed Eng*, vol. 50, no. 4, 2003.

- [14] "Advances in Network Electrophysiology i."2019.
- [15] J. Müller *et al.*, "High-resolution CMOS MEA platform to study neurons at subcellular, cellular, and network levels," *Lab Chip*, vol. 15, no. 13, 2015.
- [16] "Al_Abed_2022_J._Neural_Eng._19_056031".2022.
- [17] R. M. Almasri *et al.*, "Emerging Trends in the Development of Flexible Optrode Arrays for Electrophysiology."2022.
- [18] R. M. Almasri *et al.*, "Impedance Properties of Multi-Optrode Biopotential Sensing Arrays," *IEEE Trans Biomed Eng*, vol. 69, no. 5, 2022.
- [19] S. Addanki, I. S. Amiri, and P. Yupapin, "Review of optical fibers-introduction and applications in fiber lasers," *Results Phys*, vol. 10, Sep. 2018.
- [20] R. Zhang *et al.*, "Advanced liquid crystal-based switchable optical devices for light protection applications: principles and strategies," *Light: Science and Applications*, vol. 12, no. 1. Springer Nature, 2023.
- [21] J.-H. Lee, H.-S. Lee, B.-K. Lee, W.-S. Choi, H.-Y. Choi, and J.-B. Yoon, "Simple liquid crystal display backlight unit comprising only a single-sheet micropatterned polydimethylsiloxane (PDMS) light-guide plate," 2007.
- [22] Y. T. Kim, S. Hwang, J. H. Hong, and S. D. Lee, "Alignment layerless flexible liquid crystal display fabricated by an imprinting technique at ambient temperature," *Appl Phys Lett*, vol. 89, no. 17, 2006.
- [23] A. Yu, I. Roes, A. Davies, and Z. Chen, "Ultrathin, transparent, and flexible graphene films for supercapacitor application," *Appl Phys Lett*, vol. 96, no. 25, 2010.
- [24] Z. Yin *et al.*, "Organic photovoltaic devices using highly flexible reduced graphene oxide films as transparent electrodes," *ACS Nano*, vol. 4, no. 9, 2010.
- [25] M. Irimia-Vladu, "'Green' electronics: Biodegradable and biocompatible materials and devices for sustainable future," *Chemical Society Reviews*, vol. 43, no. 2. Royal Society of Chemistry, 2014.

- [26] P. Single and J. Scott, "Cause of pulse artefacts inherent to the electrodes of neuromodulation implants," *IEEE Transactions on Neural Systems and Rehabilitation Engineering*, vol. 26, no. 10, 2018.
- [27] C. L. Tao *et al.*, "Differentiation and characterization of excitatory and inhibitory synapses by cryo-electron tomography and correlative microscopy," *Journal of Neuroscience*, vol. 38, 2018.
- [28] Y. Nie *et al.*, "Real-time removal of stimulation artifacts in closed-loop deep brain stimulation," *J Neural Eng*, vol. 18, no. 6, 2021.
- [29] M. A. Klados, C. Papadelis, C. Braun, and P. D. Bamidis, "REG-ICA: A hybrid methodology combining Blind Source Separation and regression techniques for the rejection of ocular artifacts," in *Biomedical Signal Processing and Control*, 2011.
- [30] X. Jiang, G. Bin Bian, and Z. Tian, "Removal of artifacts from EEG signals: A review," *Sensors (Switzerland)*, vol. 19, no. 5. MDPI AG, 2019.
- [31] J. Li, X. Liu, W. Mao, T. Chen, and H. Yu, "Advances in Neural Recording and Stimulation Integrated Circuits," *Frontiers in Neuroscience*, vol. 15. Frontiers Media S.A., 2021.
- [32] "GRANT PROPOSAL-IDEAS GRANTS FUNDING COMMENCING 2024 Application ID: APP2030570 CIA Surname: Aplin."2024.
- [33] J. A. Sahel *et al.*, "Partial recovery of visual function in a blind patient after optogenetic therapy," *Nat Med*, vol. 27, no. 7, 2021.
- [34] M. Muralidharan *et al.*, "Neural activity of functionally different retinal ganglion cells can be robustly modulated by high-rate electrical pulse trains," *J Neural Eng*, vol. 17, no. 4, 2020.
- [35] N. G. Hatsopoulos and J. P. Donoghue, "The science of neural interface systems," *Annual Review of Neuroscience*, vol. 32. pp. 249–266, 2009.